ETH
Eidgenössische Technische Hochschule Zürich
Swiss Federal Institute of Technology Zurich

IAC Institute for Atmospheric and Climate Science

PSI

Master Thesis

Photochemical reduction of Iodate through Iron-containing Complexes in Secondary Organic Aerosol from Monoterpene Oxidation

David Immanuel Tschan[1]

[1]Institute of Amtospheric and Climate Science,
Department of Environmental Sciences, ETH Zürich

Student-ID: 20-914-180
E-Mail: datschan@student.ethz.ch

Supervised By:

Prof. Dr. Markus Ammann[2]
Nicole Carina Leemann[2]

[2]Laboratory of Atmospheric Chemistry,
Paul Scherrer Institut PSI

20.05.2026 — 02.12.2026

Title page image courtesy to Alessio Soggetti from unsplash.com (accessed on 26.05.2026 10:00).
The font used in figures including technical drawings (figs. ...) was accessed from https://github.com/hikikomori82/osifont on 06.08.2026 09:25 and is distributed under the GNU GPL V3 + FE license.
The beaker in figure 2.3 was adapted from "Diogo Losch De Oliveira (2026). Beakers [Illustration]. CC-BY 4.0. SciDraw.io. https://scidraw.io/drawing/beakers-ba8583ed" (accessed 10.08.2026 16:16)

“ You’ve gotta dance like there’s nobody watching, love like you’ll never be hurt, sing like there’s nobody listening, and live like it’s heaven on earth. ” (William W. Purkey, 2003)

Contents

1 Introduction **8**
- 1.1 Monoterpenes in the atmosphere . . . 8
- 1.2 Iodine in the atmosphere . . . 8
  - 1.2.1 Iodine cycle and sources of atmospheric iodine . . . 8
  - 1.2.2 Atmospheric chemistry of iodine . . . 8
- 1.3 Organic iron complexes and iodine . . . 8
- 1.4 Current state of research . . . 8
- 1.5 Relevant instrumentation . . . 8

2 Methods **9**
- 2.1 SOA filter production in oxidation flow reactor (OFR) . . . 9
  - 2.1.1 Procedure . . . 10
  - 2.1.2 Oxidation Flow Reactor . . . 11
  - 2.1.3 Scanning Mobility Particle Sizer . . . 11
  - 2.1.4 Ozone analyser and other instrumentation . . . 11
- 2.2 Filter extraction and total organic carbon (TOC)-analysis . . . 11
  - 2.2.1 Preparation . . . 11
  - 2.2.2 Extraction . . . 12
  - 2.2.3 Calibration . . . 12
  - 2.2.4 Measurements . . . 12
- 2.3 CWFTR experiments . . . 12
  - 2.3.1 Preparation . . . 12
  - 2.3.2 Coating solution Preparation . . . 12
  - 2.3.3 Procedure . . . 12
- 2.4 Data analysis . . . 12

3 Results **13**
- 3.1 OFR- and TOC Data . . . 13

4 Introduction **17**
- 4.1 Iodine in the environment . . . 17
- 4.2 Iodine Chemistry in the Atmosphere . . . 18
- 4.3 Reduction of Iodate . . . 19
- 4.4 Reduction of Iodate: Proxies for Secondary Organic Aerosol . . . 21

5 Introduction **23**
- 5.1 Iodine in the environment . . . 23
- 5.2 Iodine Chemistry in the Atmosphere . . . 24
- 5.3 Reduction of Iodate . . . 25
- 5.4 Reduction of Iodate: Proxies for Secondary Organic Aerosol . . . 27

6 Acknowledgements **29**

Bibliography **30**

Acronyms **33**

List of Symbols **34**

List of Species **35**

Glossary **36**

Index **37**

List of Tables

2.1 Overview over filters and flows 11

List of Figures

2.1 Overview over Workflow 9
2.2 Overview over OFR Flowchart 10
2.3 Procedure to create solutions 12

3.1 Data for α-pinene filters 13
3.2 Data for Limonene filters 14
3.3 Data for β-pinene filters 15
3.4 Correlation diagrams between volatile organic compound (VOC) mass flows and ozone (O_3) concentrations. 16

1 Introduction

1.1 Monoterpenes in the atmosphere

The biosphere of Earth emits large quantities of VOCs. The natural flux of VOCs to the atmosphere exceeds the anthropogenic one, and accounts for 75…90 % of the total VOC flux (Messina et al., 2016). Due to their biogenic origin, these latter VOCs are often referred to as biogenic volatile organic compounds (BVOCs).

1.2 Iodine in the atmosphere

1.2.1 Iodine cycle and sources of atmospheric iodine

1.2.2 Atmospheric chemistry of iodine

1.3 Organic iron complexes and iodine

1.4 Current state of research

1.5 Relevant instrumentation

2 Methods

We use a sequential workflow outlined in figure 2.1. It consists of the following steps:

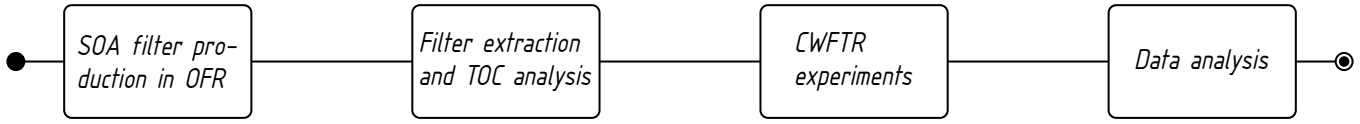


FIGURE 2.1: Overview over Workflow. The initial step consists of producing a filter containing VOC in the OFR, which is subsequently extracted to produce a solution.

1. **Secondary organic aerosol (SOA) filter production in OFR**: Within the OFR, we produce SOA through the reaction of a VOC with ozone. The resulting SOA is collected on a filter. The detailed procedure is outlined in section 2.1.
2. **Filter extraction and TOC analysis**. The filters produced in the previous step are extracted into aqueous solution and TOC is measured as a proxy for sample content of organics. This is outlined in detail in section 2.2.
3. **CWFTR experiments**. In this step, the solutions from the extracted filters are mixed with iron and iodide (I^-). Using such solutions, flow tubes are coated and the products of the reaction of their film with ozone are measured in a BTOF CIMS (BTOF-CIMS). The exact methodology is described in section 2.3
4. **Data Analysis**. In this step, the data from the BTOF-CIMS are analysed using *IGOR Pro* and *Python*. Details are available in section 2.4.

2.1 SOA filter production in OFR

An overview over the setup for filter production is displayed in figure 2.2. Molecular oxygen (O_2) and molecular nitrogen (N_2) from the in-house gas connection at Paul-Scherrer Institute (PSI) are first mixed at controlled ratios and guided inton the flow tube of the OFR. Usually, $\overset{*}{V}_{N_2} = 3.95\,\mathrm{L\,min^{-1}}$ and $\overset{*(3)}{V}_{O_2} = 1.05\,\mathrm{L\,min^{-1}}$ was set, giving a relative fraction of $N_2 : O_2 \approx 0.79 : 0.21$, which is close to atmospheric comoposition. This was achieved through the mass flow controllers (MFCs) 2 (for molecular nitrogen) and 3 (for molecular oxygen), respectively (see also figure 2.2). MFC 1 was used to control the flow of molecular nitrogen through a glass bottle containing VOC, with a value set at $\overset{*}{V}_{VOC} = 0.04\,\mathrm{L\,min^{-1}}$. In order to inhibit diffusion of VOC into the OFR, a plug valve (PV1) was installed on the VOC input line just before the OFR. Finally, MFC 4 was used to control the flow of molecular oxygen into the ozone generator, where molecular oxygen reacted with UV light to produce ozone, as in reaction below:

$$O_2 + h\nu \longrightarrow 2\,O(^1D)^{\bullet} \qquad \text{[R2.1.1]}$$

For this, MFC 4 was set to provide a flow of $\overset{*(4)}{V}_{O_2} = 3\,\mathrm{L\,min^{-1}}$ to the ozone generator. Without any additional measures, this molecular oxygen flow is efficiently converted into ozone by the generator, such that concentrations in excess $\chi_{O_3} \approx 100\,\mathrm{ppm}$ are reached within the OFR. In order to decrease ozone levels within the OFR, a pump was installed that pumped a flow of $\overset{*}{V}_P \approx 2.2\,\mathrm{L\,min^{-1}}$ of generated

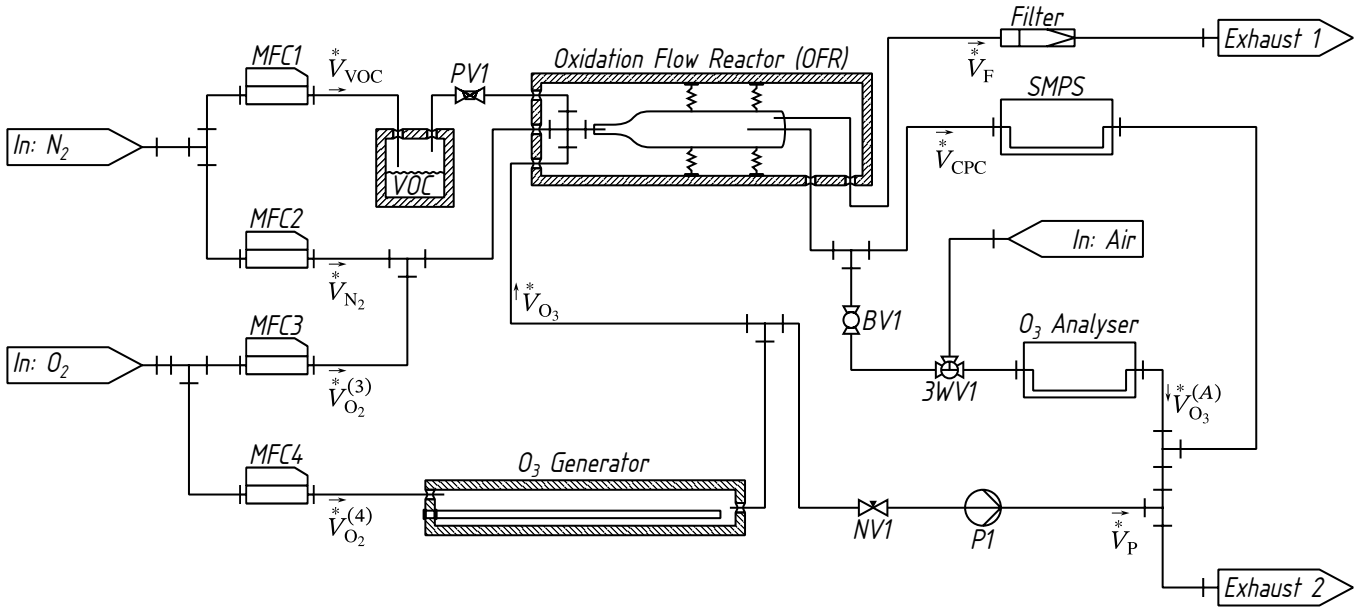


FIGURE 2.2: Overview over OFR Flowchart. Flow Chart displaying the functionality of the OFR Setup, including various flows, instruments, diverse valves and other things.

ozone into exhaust 2, such that steady-state concentrations of ozone within the OFR were not usually in excess of ≈ 70 ppm. The flow rate of the pump was adjusted using a needle valve (NV1). This was done once before the start of experiments, and the valve setting was not changed throughout experiments. Within the OFR, thus, the flows of VOC (on its N_2 carrier gas), "air" (with $N_2 : O_2 = 0.79 : 0.21$) and ozone (at $\dot{V}^*_{O_3} \approx 0.8\,\mathrm{L\,min^{-1}}$) converge. Here, VOC is oxidised by ozone into oxygenated volatile organic compounds (OVOCs) and low-volatility organic compounds (LVOCs). These LVOCs condense into SOA.

Two lines exit the OFR: One that takes an air sample from within the middle of the flow tube, where the flow is nearly laminar, and another one consisting of four different outlets at the flow tubes' rear end that converge into a single outlet line. The latter line is connected to a filter holder through which a flow of product gases $\dot{V}^*_F \approx 4.5\,\mathrm{L\,min^{-1}}$ is guided into exhaust 1 — it is here that SOA is collected: within the filter holder, a Nylon filter with pore size 0.45 µm is installed, on which SOA is collected. The other line is guided into the scanning mobility particle sizer (SMPS) and the ozone analyser. Downstream of those instruments, the flow through the former line is converging again, and sucked into exhaust 2 along with excess ozone from the pump. The SMPS allows for an online measurement of particle size, and is described in detail in section 2.1.3. Using a ball valve (BV1), the line can be opened or closed towards the ozone analyser: if BV1 is closing the OFR outlet flow towards the analyser, a three-way-valve (3WV1) allows for the ozone analyser to sample ambient air. In normal operation, BV1 is open and 3WV1 closes off the system towards the ambient. In this configuration, a flow of $\dot{V}^*_{CPC} \approx 0.3\,\mathrm{L\,min^{-1}}$ is guided into the SMPS and a flow of $\dot{V}^{*(A)}_{O_3} \approx 1\,\mathrm{L\,min^{-1}}$ flows through the ozone analyser.

2.1.1 Procedure

A detailed methodological procedure is available in appendix **??**. Throughout the experiments, SMPS data was collected within ≈ 60 (this number varied across experiments) samples, each of which constitutes of aggragating data for 180 s. Briefly, the following steps need to be undertaken:

1. All lines are checked and it is ensured that SMPS and ozone analyser are ready for data logging;
2. The ozone analyser and condensation particle counter (CPC) are switched on so that they can warm up.
3. Flows are set at $\dot{V}^*_{N_2} = 3.95\,\mathrm{L\,min^{-1}}$, $\dot{V}^{*(3)}_{O_2} = 1.05\,\mathrm{L\,min^{-1}}$ and $\dot{V}^{*(4)}_{O_2} = 1.05\,\mathrm{L\,min^{-1}}$. The ozone excess pump is switched on.
4. Ozone data logging is started, filter holder is loaded with filter and attached to the system.

5. Start logging SMPS data and turn on ozone generator. Let the system equilibrate for 45 min (for 15 samples)

6. Just before ($\approx$ 10 s) 15 samples have been recorded, open the VOC valve (PV1). At the onset of the next sample, set $\overset{*}{V}_{\mathrm{VOC}} = 0.04\,\mathrm{L\,min^{-1}}$. Let the system run for 1 h (for 20 samples).

7. When 1 h has passed, and at the onset of the sample subsequent to the ones recorded in the last step, reset $\overset{*}{V}_{\mathrm{VOC}} = 0\,\mathrm{L\,min^{-1}}$. Within $\approx$ 10 s, close the VOC valve (PV1). Let the system equilibrate for 30 min.

2.1.2 Oxidation Flow Reactor

2.1.3 Scanning Mobility Particle Sizer

The aerosol concentration is measured using a SMPS, which in turn consists of a differential mobility analyser (DMA) and a CPC, arranged in series.

$$m_{\mathrm{F}} = \int_{t_{\mathrm{in}}}^{t_{\mathrm{out}}} \overset{*}{m}\,\mathrm{d}t \approx \sum_{\mathrm{Samples}} \overset{*}{m}_i \Delta t_i \tag{2.1}$$

2.1.4 Ozone analyser and other instrumentation

TABLE 2.1: Overview over filters and flows

Date	$\overset{*}{V}_{\mathrm{VOC}}$	$\overset{*}{V}_{\mathrm{N_2}}$	$\overset{*}{V}^{(3)}_{\mathrm{O_2}}$	$\overset{*}{V}^{(4)}_{\mathrm{O_2}}$	$\overset{*}{V}_{\mathrm{P}}$	$\overset{*}{V}_{\mathrm{O_3}}$	$\overset{*}{V}_{\mathrm{F}}$	$\overset{*}{V}_{\mathrm{CPC}}$	$\overset{*}{V}^{(A)}_{\mathrm{O_3}}$
	$\mathrm{m^3\,s^{-1}}$	$\mathrm{m^3\,s^{-1}}$	$\mathrm{m^3\,s^{-1}}$	$\mathrm{m^3\,s^{-1}}$	$\mathrm{m^3\,s^{-1}}$	$\mathrm{m^3\,s^{-1}}$	$\mathrm{m^3\,s^{-1}}$	$\mathrm{m^3\,s^{-1}}$	$\mathrm{m^3\,s^{-1}}$
a	a	a	a	a	a	a	a	a	a

2.2 Filter extraction and TOC-analysis

$$?? := ?? - ?? \tag{2.2}$$

2.2.1 Preparation

Preparation for TOC measurements essentially consists in cleaning glassware required for analysis and extraction. This is rather not straightforward, and two procedures need to be distinguished: a special procedure before the campaign to obtain a standard of cleanliness, and a procedure during the campaign to retain the obtained standard.

Intial Glassware Cleaning

During initial cleaning, non-purgeable organic carbon (NPOC)?? of glassware is tested. Glassware is considered clean if $?? < 0.1\,\mathrm{mg\,L^{-1}}$.

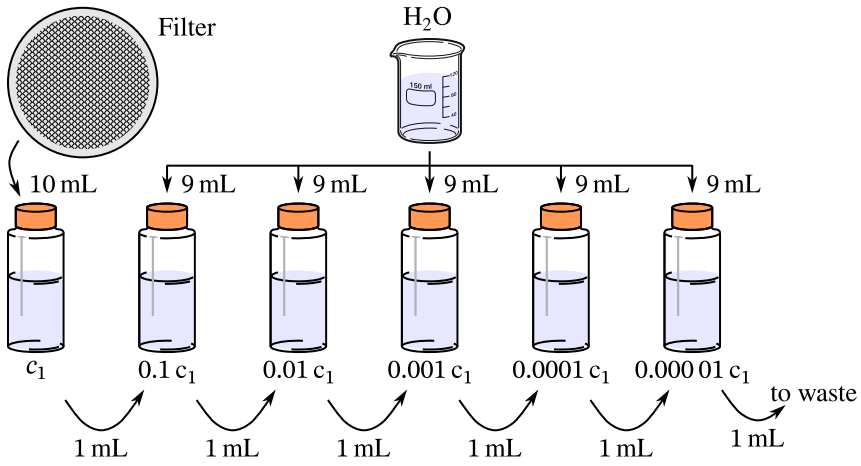


FIGURE 2.3: Procedure to create solutions. Beaker apapted from: Diogo Losch De Oliveira (2026). Beakers [Illustration]. CC-BY 4.0. SciDraw.io. https://scidraw.io/drawing/beakers-ba8583ed, accessed 10. August 16:16

Subsequent Glassware cleaning

2.2.2 Extraction

2.2.3 Calibration

2.2.4 Measurements

2.3 CWFTR experiments

2.3.1 Preparation

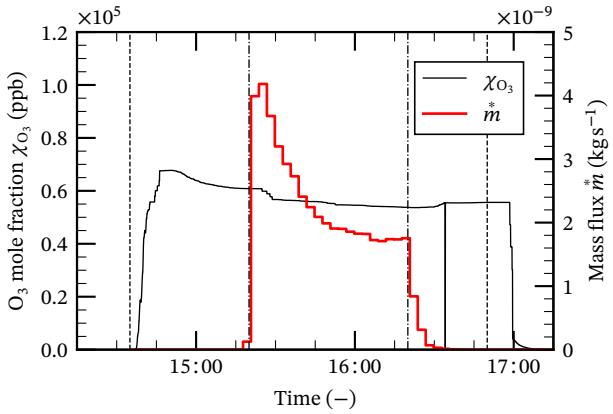
2.3.2 Coating solution Preparation

2.3.3 Procedure

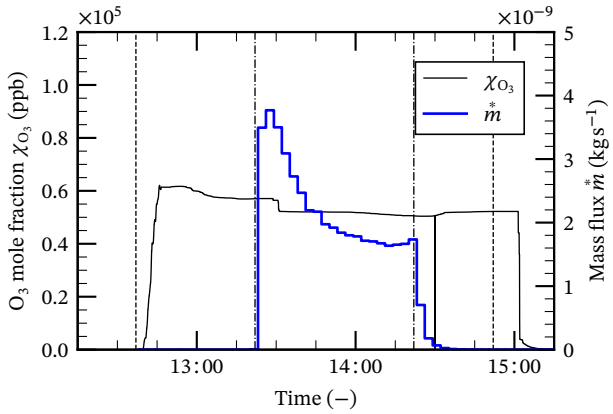
2.4 Data analysis

3 Results

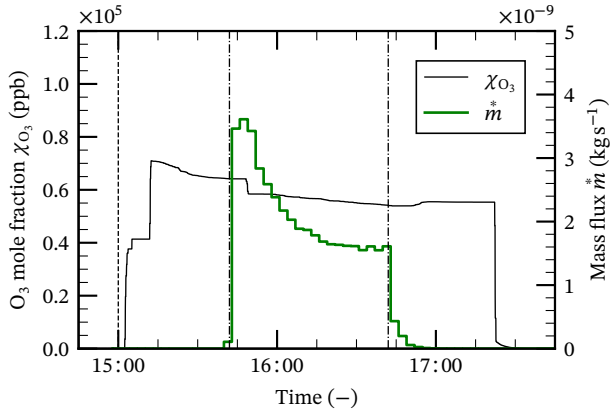
3.1 OFR- and TOC Data



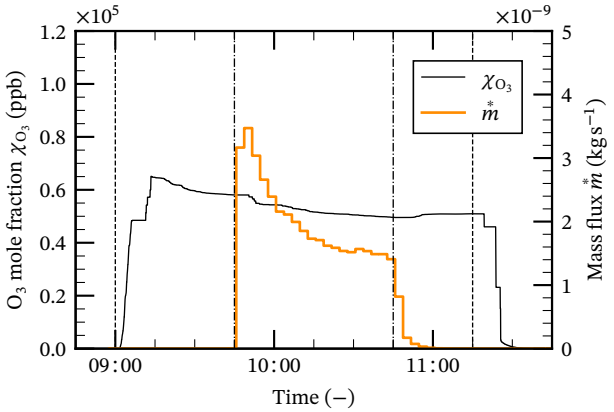
(a) Data for filter in set 2 experiment 14 (03.09.2026).



(b) Data for filter in set 2 experiment 15 (04.09.2026).



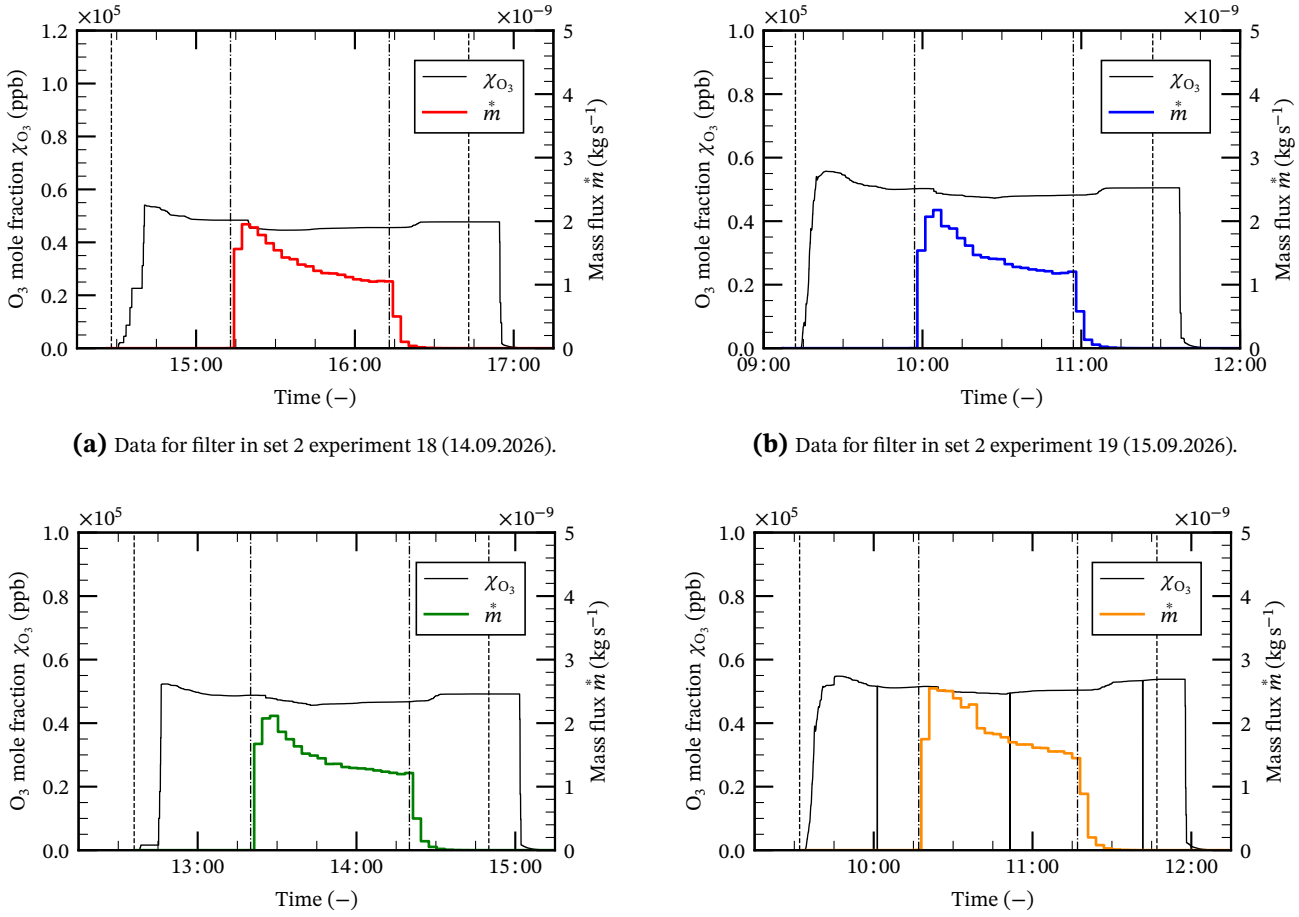
(c) Data for filter in set 2 experiment 16 (10.09.2026).



(d) Data for filter in set 2 experiment 17 (14.09.2026).

FIGURE 3.1: Data for α-pinene filters. **(a)**: Data for the filter from set 2 experiment 14 from 03.09.2026. Dotted lines indicate activating and deactivating the Ozone source, respectively. Dash-dotted lines indicate the activation and deactivation of α-pinene flow. **(b) — (d)**: As in (a), but for set 2 experiments 15, 16 and 17, respectively.

This is some reference to fig. 3.2, fig. 3.2a and some reference to fig. (c).



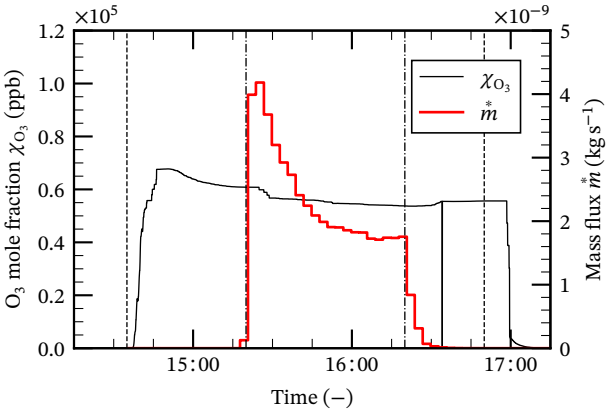
(a) Data for filter in set 2 experiment 18 (14.09.2026).

(b) Data for filter in set 2 experiment 19 (15.09.2026).

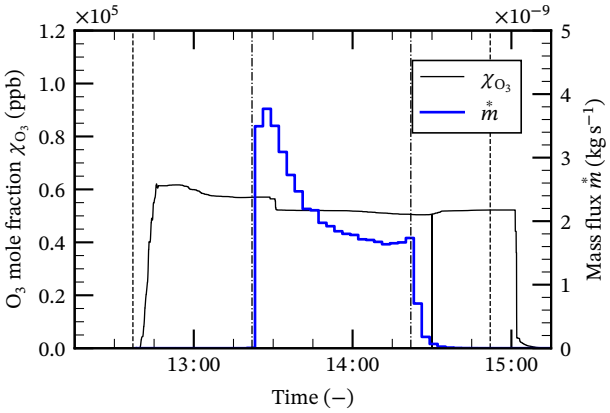
(c) Data for filter in set 2 experiment 20 (15.09.2026).

(d) Data for filter in set 2 experiment 21 (16.09.2026).

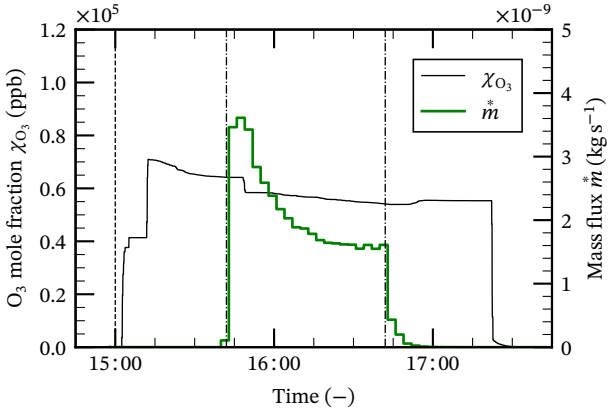
FIGURE 3.2: Data for Limonene filters. **(a)**: Data for the filter from set 2 experiment 22 (02.09.2026). Dotted lines indicate activating and deactivating the Ozone source, respectively. Dash-dotted lines indicate the activation and deactivation of Limonene flow. **(b) — (d)**: as in (a), but for set 2 experiments 19, 20 and 21, respectively.



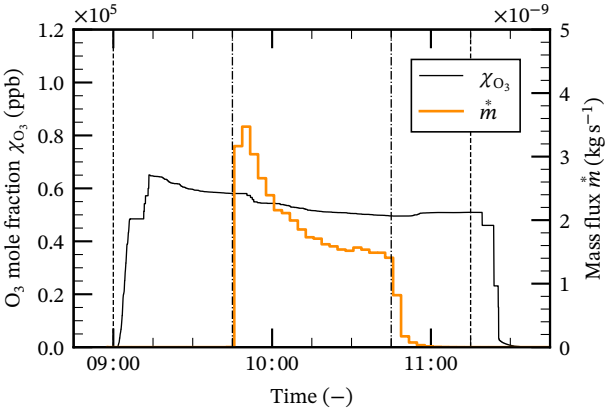
(a) Data for filter in set 2 experiment 14 from 02.09.2026.



(b) Data for filter in set 2 experiment 15 from 03.09.2026.

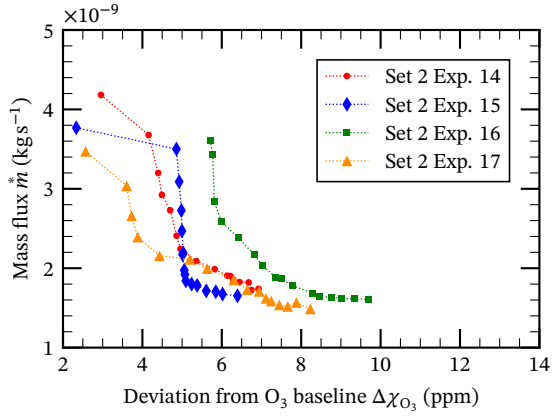


(c) Data for filter in set 2 experiment 16 from 04.09.2026.

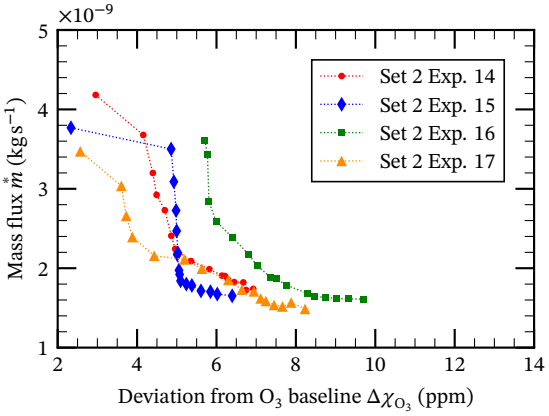


(d) Data for filter in set 2 experiment 17 from 04.09.2026.

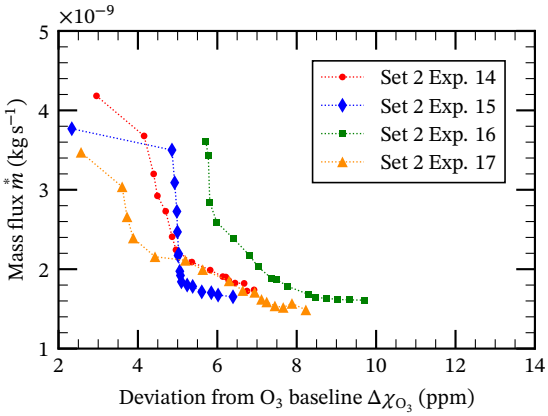
FIGURE 3.3: Data for β-pinene filters. **(a)**: Data for the filter from set 2 experiment 18 (02.09.2026). Dotted lines indicate activating and deactivating the Ozone source, respectively. Dash-dotted lines indicate the activation and deactivation of β-pinene flow. **(b) — (d)**: as in (a), but for set 2 experiments 19 (03.09.2026), 20 (22.22.2222) and 21 (22.22.2222).



(a) Data for filter in set 2 experiment 14 from 02.09.2026.



(b) Data for filter in set 2 experiment 15 from 03.09.2026.



(c) Data for filter in set 2 experiment 16 from 04.09.2026.

FIGURE 3.4: Correlation diagrams between VOC mass flows and ozone concentrations. **(a)**: Filter mass flux $\dot{m}$ in dependency of ozone concentration for α-pinene filters. Deviation from ozone baseline is computed as the average Ozone values for 5 min before α-pinene is switched on. **(c)**: As in (a), but for Limonene. **(b)**: As in (a), but for β-pinene.

4 Introduction

Iodine is the heaviest stable halogen element with atomic number 53. It has an average atomic weight of 126.904 u and forms a semi-lustrous solid under standard conditions (here 273.15 K and 1 bar, see Calvert (1990)) (Kaiho, 2015). Its melting and boiling points are 114 °C and 184 °C, respectively, and its vapour pressure is 0.031 kPa and 9.17 kPa at 25 °C and 113.6 °C, respectively (Kaiho, 2015). The atomic radius of iodine is 140 pm and its first ionisation energy is 1015 kJ mol^{-1} (Kaiho, 2015). Iodine is important in the enviornment: in the atmosphere, it influences the chemistry of ozone and important radical species, and it may be cause the formation of particles that may act as nuclei for aerosol or clouds (Saiz-Lopez, Plane, et al., 2012). The former is important for the capability of the atmophere to oxidise and remove species emitted to it, while the latter is important because of its effect on radiative equilibrium of Earth.

4.1 Iodine in the environment

Iodine is litophilic and incompatible in Earth's astenosphere, and therefore concentrated in oceans and surface sediments (Kendrick, 2024). Marine sediments constitute the largest iodine reservoir (Kendrick, 2024) with much higher concentrations of 20…600 mg kg^{-1} compared to soil- (0.5…20 mg kg^{-1}) or rock (0.08…0.5 mg kg^{-1}) concentrations (Whitehead, 1984). Sedimented iodine may be recycled into the oceans through sedimentary brines (Muramatsu, Fehn, et al., 2001; Muramatsu, Yoshida, et al., 2004) around techtonically active subduction zones (Carrano et al., 2020) through diagenesis processes involving thermal decompostion or microbiological reduction of buried organic matter (Kendrick, 2024; Muramatsu, Fehn, et al., 2001). Consequently, iodine concentrations in the oceans are approximately 45…60 µg L^{-1} (Whitehead, 1984), mostly in the form of iodate (IO_3^-), the thermodynamically most stable state of iodine in aqueous solution (Fuge et al., 2015). However, iodate exhibits a nutrient-like profile (Carrano et al., 2020) being depleted at the surface, whereas iodide is enriched in the surface (Elderfield et al., 1980). Similarly, organic matter is enriched in the surface, so that the existence of some iodinated organics may be presumed (Saiz-Lopez, Plane, et al., 2012). Within the oceans, iodine is incorporated preferrentially in organic matter (Kendrick, 2024) by micro- and macroalgae, and aerobic bacteria (L. Carpenter, 2015): through faciliated diffusion (see detailed descriptions in Küpper et al. (2008), Winter et al. (2009), and Amachi (2008)), cells store iodine as I^-(aq) or associated to organic molecules (Küpper et al., 2008; Amachi, 2008). Iodide within the cell interior may act as an antioxidant (Küpper et al., 2008): upon oxidative stress, the iodide reservoir is mobilised and cells emit I^-(aq) and a range of volatile organic iodine compounds (VOICs) (Küpper et al., 2008; L. Carpenter, 2015) that may volatilise to the atmosphere. Analogously, when oxidative stress occurs during air exposure at low tide, the hetergeneous surface reaction of iodide and ozone at the sea-water interface produces hypoiodous acid (HOI), molecular iodine (I_2) and iodine monoxide radicals ($IO^\bullet$) directly emitted to the atmosphere (L. Carpenter, 2015; Palmer et al., 2005; Liu et al., 2001; Sakamoto et al., 2009; Hayase et al., 2010; He et al., 2021). It is currently thought that the biggest source of inorganic iodine to the atmosphere is hypoiodous acid produced via the same pathway, exceeding the emissions of molecular iodine by one order of magnitude (L. J. Carpenter et al., 2013). Nevertheless, the atmospheric iodine budget is currently not well-constrained (Saiz-Lopez, Plane, et al., 2012). VOICs (notably CH_3I) and inorganic iodine species (HOI, I_2, $IO^\bullet$) emitted from the oceans constitute the biggest source of iodine to the atmosphere (L. Carpenter, 2015; L. J. Carpenter et al., 2013), with estimated input $\approx$ 550 Gg yr^{-1} (Saiz-Lopez, Plane, et al., 2012). Most VOICs are photolabile with lifetimes on the order of minutes to days (Bloss et al., 2001). Other natural sources of iodine to the am-

tosphere include soils and plants (Whitehead, 1984; L. Carpenter, 2015; Fuge et al., 2015), terrestrial water systems (Whitehead, 1984), and volcanoes or salt lakes (L. Carpenter, 2015). The additional input from terrestrial sources into the atmosphere is $\approx 80 \ldots 110\,\mathrm{Gg\,yr^{-1}}$ (Saiz-Lopez, Plane, et al., 2012). Anthropogenic sources include direct emissions from fossil fuel burning (Fuge et al., 2015) and pesticide use (Zheng et al., 2003; Whitehead, 1984). There are indirect anthropogenic effects as well: ice core data indicates that the sea-air flux of iodine has tripled between 1950 and 2010 as a consequence of increased anthropogenic ozone pollution of the troposphere (Cuevas et al., 2018). Sinks of atmospheric iodine include wet- and dry deposition (Fuge et al., 2015), and direct uptake through plants (Fuge et al., 2015). Overall, this leads to boundary layer mixing ratios of $\chi_{\mathrm{I_2(g)}} \leq 93\,\mathrm{pptv}$ (L. Carpenter, 2015), $\chi_{\mathrm{IO^{\cdot}(g)}} \leq 3 \ldots 20\,\mathrm{pptv}$ (L. Carpenter, 2015), $\chi_{\mathrm{HOI(g)}} \leq 1\,\mathrm{pptv}$ (He et al., 2021) and $\chi_{\mathrm{I^{\cdot}(g)}} \leq 0.1 \ldots 22\,\mathrm{pptv}$ (L. Carpenter, 2015; He et al., 2021).

4.2 Iodine Chemistry in the Atmosphere

The importance of the marine iodine source is likely also reflected in aerosol composition: above marine areas, aerosol is enriched in iodine relative to seawater content by a factor of 100…1000 (L. Carpenter, 2015). Iodine may be transported into the aerosol phase through bubble-bursting of iodine-rich surface ocean waters (Saiz-Lopez, Plane, et al., 2012), or through the formation of aerosol via iodine oxide particles (IOPs) (O'Dowd et al., 2002). Likely, low-volatility iodinated organics may also condense into the aerosol phase. Overall, various iodinated species may be present in aerosol including iodide, iodate, hypoiodous acid and soluble organic iodine (SOI) (Saiz-Lopez, Plane, et al., 2012). Saiz-Lopez, Plane, et al. (2012) and Gilfedder et al. (2008) report that SOI is very frequent in aerosol and may constitute the largest reservoir of iodine in aerosol. There appear to be two principal pathways of SOI accomodation: direct accumulation from sea spray enriched in iodinated organics, and the reaction of hypoiodous acid with aerosol organics. Hypoiodous acid may also be highly reactive towards other species, likely due to its affinity for nucelophilic attacks on susceptible species. In general however, hypoiodous acid or other likewise reduced iodine species such as iodide should be oxidised to iodate (Gilfedder et al., 2008), the thermodynamically most stable form of iodine in aqueous solution. Consequently, the accumulated form of iodine in condensed aerosol phases is often thought to be iodate (Gilfedder et al., 2008; Saiz-Lopez, Plane, et al., 2012). However, observations in the troposphere indicate higher aerosol contents of iodide than iodate (Gilfedder et al., 2008), or high variability in the iodide/iodate ratio (Saiz-Lopez, Plane, et al., 2012). This indicates the presence of a mechanism reducing iodate in the troposphere.

Hetergeneous aerosol chemistry of iodine is closely linked to homogeneous chemistry of iodine through many iodine species. Generally, atmospheric iodine chemistry is initiated mostly through reactive iodine species (RIS) such as iodine radicals ($\mathrm{I^{\cdot}}$) or iodine monoxide radicals. Briefly, homogeneous iodine chemistry involves catalytic destruction of troposheric ozone via various pathways involving hydrogen oxide radicals (HO_x) and nitrous oxides (NO_x) as well as other halogen atoms in the atmosphere (Saiz-Lopez and Von Glasow, 2012). This process is photochemically driven and initiated with $\mathrm{IO^{\cdot}}$ and $\mathrm{I^{\cdot}}$. Saiz-Lopez and Von Glasow (2012) have outlined the mechanism: the intial step is the production of iodine radicals from VOICs (RI_n) or molecular iodine. The iodine radicals react with ozone to produce iodine monoxide radicals that in turn recombine to again produce iodine radicals:

$$\mathrm{RI(g)} + h\nu \longrightarrow \mathrm{R^{\cdot}(g)} + \mathrm{I^{\cdot}(g)} \qquad \text{[R4.2.1]}$$

$$\mathrm{I_2(g)} + h\nu \longrightarrow 2\,\mathrm{I^{\cdot}(g)} \qquad \text{[R4.2.2]}$$

$$\mathrm{I^{\cdot}(g)} + \mathrm{O_3(g)} \longrightarrow \mathrm{IO^{\cdot}(g)} + \mathrm{O_2(g)} \qquad \text{[R4.2.3]}$$

$$2\,\mathrm{IO^{\cdot}} \longrightarrow 2\,\mathrm{I^{\cdot}(g)} + \mathrm{O_2(g)} \qquad \text{[R4.2.4]}$$

The net outcome is ozone destruction with $2\,\mathrm{O_3(g)} \longrightarrow 3\,\mathrm{O_2(g)}$, although reaction 5.2.4 has other channels that may involve HO_x and

NO_x cycles. Importantly, the iodine monoxide radical has a lifetime against photolysis in the boundary layer on the order of seconds (Bloss et al., 2001). Likewise, the effective lifetime of iodine radical species (I_x) against uptake in aerosol is on the order of hours (Dix et al., 2013): sustained presence of iodine monoxide radicals in the atmosphere therefore requires an effective recycling mechanism for $IO^{\bullet}$.

Additionally, iodine may be involved in the oxidation of atmospheric organic molecules or mercury, allowing the latter to enter the food chain as highly poisonous methylmercury (Steffen et al., 2008; Saiz-Lopez and Von Glasow, 2012; Saiz-Lopez, Plane, et al., 2012), and likely leading to enhanced condensation of organics into the aerosol phase through the former. Further, through formation of IOPs, iodine oxides may lead to the production of ultrafine aerosol particles (UFAPs) (L. Carpenter, 2015). Volatile species may condense on UFAPs that can grow up to the point of becoming cloud condensation nuclei (CNN) (Saiz-Lopez, Plane, et al., 2012). Recent evidence shows that nucleation via iodine oxoacids to produce IOPs is highly efficient and sometimes competitive with sulfuric acid-ammonium driven nucleation (He et al., 2021). Moreover, heterogeneous iodine chemistry on pre-existing frozen or liquid salt particles may lead to sudden increases in gas phase iodine species (Saiz-Lopez and Von Glasow, 2012). Importantly, the reaction of bromide (Br^-) with ozone on frozen salt solutions occurs in the brine pertaining to the bulk ice phase, rather than *within* the bulk ice phase (Oldridge et al., 2011): such brines are formed when freezing solutions exclude solutes — the heterogeneous reaction of ozone with iodide on frozen aerosol is here assumed to behave similarly. In other words, the heterogeneous reaction of ozone with aerosol surfaces is assumed to be similar for frozen and liquid aerosol particles.

Other heterogeneous effects may lead to substantial iodine emissions through the reaction of ozone with dissolved iodide in ocean and aerosols (Palmer et al., 2005; Liu et al., 2001; Sakamoto et al., 2009; Hayase et al., 2010). In the upper troposphere and lower stratosphere, heterogeneous recycling of iodine species is highly important: Model calculations by Saiz-Lopez, Baidar, et al. (2015) show that from the lower troposphere, convection may transport inorganic- and organic iodine species to the lower stratosphere, causing a total inorganic iodine (I_y) injection of 0.25…0.7 pptv (Saiz-Lopez, Baidar, et al., 2015). Measurements by Koenig, Baidar, et al. (2020) are in agreement with this, indicating an injection of 0.77 ± 0.10 pptv of I_y into the lower stratosphere. Associated therewith is a mixing ratio of $\chi_{IO^{\bullet}(g)} = 0.06 \pm 0.03$ pptv even for aged stratospheric air. Koenig, Baidar, et al. (2020) also observed that increases in altitude across the troposphere are associated with (1) an increase in particulate iodine and a decrease in gas phase iodine; and (2) a shift of iodide-iodate speciation in the condensed phase towards iodate. Simulations could reproduce observed $\chi_{IO^{\bullet}(g)}$ only when a recycling scheme for iodine on ice particles was applied, and when the proper partioning between condensed- and gas phase was applied. This indicates that, as for the troposphere, a recycling mechanism producing gas phase iodine monoxide radicals must exist. There is also evidence that iodate should be reduced to iodide: Pillar-Little et al. (2013) have established a pathway through which iodide and ozone cause volatilization of I_2(g) and HOI(g) from watery microdroplets. However, it is still unclear *how* the necessary iodide is formed, given that most iodine should be present as iodate. Consequently, an important question to answer is: how is IO_3^- reduced to species — most likely I^- — that may, directly of after reacting, volatilise to the gas phase?

4.3 Reduction of Iodate

Saunders et al. (2012) have shown that iodate may be reduced when solutions of iodate and humic acid (HA) are irradiated with UV-A and visible (VIS) light between $\lambda \geq 310\,\text{nm}$ and $\lambda \approx 780\,\text{nm}$. The light source was filtered to exclude infra red (IR) light and lamp output below $\lambda = 310\,\text{nm}$ to simulate the UV-A-VIS solar spectrum in the lower troposphere. They found that the major product of this photochemically induced process was SOI and that the proportion of iodide in the reactant solution remained constant at approximately 20 %. Since HA is a chromophore, the suggested mechanism involves photogeneration of solvated electrons e^-(aq) that, in dependence of pH, yield hypoiodous acid: $IO_3^-(aq) + 4\,e^-(aq) + 5\,H^+(aq) \longrightarrow HOI(aq) + 2\,H_2O(aq)$. From there, SOI may be created through the

nucleophilic attack of hypoiodous acid on diphenolic functional groups (Saunders et al., 2012). Alternatively, molecular iodine may be produced through reaction 5.3.1, as described by Pillar-Little et al. (2013):

$$HOI(aq) + I^- + H^+(aq) \longrightarrow I_2(aq) + H_2O(l) \quad [R4.3.1]$$

Since molecular iodine is insoluble (Saiz-Lopez, Plane, et al., 2012), there will be volatilisation of molecular iodine to the gas phase. Overall, the mechanism suggested by Saunders et al. (2012) produces primarily hypoiodous acid molecular iodine — the production pathway of iodide has not been elucidated. The presence of iodide, however, appears necessary for the production of $I_2(g)$. It is hypothetised that iodide may be regenerated from SOI (Saunders et al., 2012; Baker, 2005). Finally, Saunders et al. (2012) have reported oscillations in the release of $I_2(g)$. This is likely associated with formation of hydrogen peroxide (H_2O_2) as a byproduct of HA photolysis (Saunders et al., 2012). Indeed, Cooper et al. (1988) have shown that hydrogen peroxide is a common product when irradiating aqueous solutions of chromophores. Given hydrogen peroxide, oscillations in I_2-IO_3^- are known as the Bray-Liebhafsky mechanism (BLM), first described by Bray (1921) and Bray and Liebhafsky (1931): hydrogen peroxide interacts with molecular iodine and iodate via

$$2\,IO_3^-(aq) + 2\,H^+(aq) + 5\,H_2O_2(aq) \rightleftharpoons I_2(aq) + 5\,O_2(g) + 6\,H_2O(l) \quad [R4.3.2]$$

$$I_2(aq) + 5\,H_2O_2(aq) \rightleftharpoons 2\,IO_3^-(aq) + 2\,H^+(aq) + 4\,H_2O(l) \quad [R4.3.3]$$

to yield a net catalytic decomposition of hydrogen peroxide via

$$2\,H_2O_2(aq) \longrightarrow 2\,H_2O(l) + O_2(g) \quad [R4.3.4]$$

The oscillation reaction has a *stable* regime — here, all species reach steady state except H_2O_2: likely, $O_2(g)$ volatilises and Le Chatelier's principle (LCP) dictates that hydrogen peroxide consequently depletes. The *unstable* regime where either reaction 5.3.2 or 5.3.3 occur preferrentially, leads to oscillations in molecular iodine and iodate. These oscillations are modulated by initial pH (Bray, 1921) and temperature. Including an organic reducing agent and a metal-ion catalyst results in the Briggs-Rauscher mechanism (BRM) after Briggs et al. (1973), elucidated by Schmitz et al. (2012): Briefly, in addition to reaction 5.3.3, the presence of some organic species $R-H_2$ will induce the following reactions:

$$H^+(aq) + IO_3^-(aq) + 2\,I_2(aq) + 5\,R{-}H_2(aq) \longrightarrow 5\,R{-}HI + 3\,H_2O \quad [R4.3.5]$$

$$H^+(aq) + IO_3^-(aq) + 2\,I_2(aq) + 5\,R{-}HI(aq) \longrightarrow 5\,R{-}I_2 + 3\,H_2O \quad [R4.3.6]$$

$$R{-}I_2 + R{-}H_2 \rightleftharpoons 2\,R{-}HI \quad [R4.3.7]$$

The backward reaction likely proceeds via the metal ion catalyst, although Schmitz et al. (2012) reported the possibility of non-catalysed pathways.

A lot has been learned so far: organic substances may lead to the reduction of iodate, via chromophore activity. Furthermore, observed oscillations in gas phase I_2 may be explained through BLM-BRM mechanisms. However, the suitability of HAs to represent organic aerosol has been questioned: Graber et al. (2006) suggested that humic-like substances found in aerosol particles may differ substantially

from humic substances found in soil. More specifically, Graber et al. (2006) argue that terrestrial sources — from which the HA used by Saunders et al. (2012) likely originate — may not be the origin of the majority of humic-like substances in aerosol. Differences may be found in terms of molecular weight, aromatic moiety content, surface properties and other properties (Graber et al., 2006). Although HAs as organics have profen useful to elucidate the mechanisms of I_2 recycling, quantitatively constraining this recycling better requires more realistic organics. Another important question to answer, therefore, is: are there proxies that represent organics in aerosol more accurately, and to which the same chromophore-dependent pathway of iodine recycling applies?

4.4 Reduction of Iodate: Proxies for Secondary Organic Aerosol

A. Guenther et al. (1995) modelled global natural VOC emissions in 1990. They found a total flux of 1150 TgC yr^{-1}, of which 44 % (503 TgC yr^{-1}) was isoprene (2-metyhl-1,3-butadiene) (CH_2=C(CH_3)−CH=CH_2) and 11 % (127 TgC yr^{-1}) were monoterpenes such as α-pinene (2,6,6-trimethylbicyclo[3.1.1]hept-2-ene). Thereof, approximately 75 % orginated from forests. In 2006, The annual atmospheric VOC injection was further specified in 2012 when A. B. Guenther et al. (2012) reported the following emissions of VOCs for the year 2000: total emissions were 1089 TgC yr^{-1}, of which isoprene emissions were 49.1 % (535 TgC yr^{-1}) and the monoterpenes α-pinene, β-pinene (6,6-dimethyl-2-methylidenebicyclo[3.1.1]heptane) and limonene (1-methyl-4-(prop-1-en-2-yl)cyclohex-1-ene) contributed 6.7 % (66.1 TgC yr^{-1}), 1.7 % (18.9 TgC yr^{-1}) and 1.0 % (11.4 TgC yr^{-1}), respectively. isoprene and monoterpene emissions are biogenic and mostly linked to vegetation — overall they contributed approximately 65 % to global VOC emissions in 2000 (A. B. Guenther et al., 2012), rendering them a major source of atmospheric VOCs.

Organic matter in aerosol is present either as primary organic aerosol (POA) or SOA. POA and SOA comprise the largest share of *fine* particles with diameters $d \leq 2.5\,\mu m$. On the other hand, large particles with diameters $d > 2.5\,\mu m$ are mostly comprised of particles formed mechanically, including soil and mineral dust, sea salt particles and plant particles (J. Ziemann et al., 2012). POA requires no chemical reactions to condense to the aerosol phase. Conversely, SOA is created when volatile precursor species are chemically altered to lower volatilities, and consequently condense to the aerosol phase. Likely, SOA constitues a large fraction of organic aerosol Bianchi et al., 2019; Hallquist et al., 2009. As a general rule of thumb, higher oxygen content of a molecule indicates *lower* volatility. Therefore, oxidation reactions are highly important in SOA formation because oxidation effectively *decreases* volatility. Recent work summarised by Bianchi et al. (2019) suggests that there exists class of of low-volatile species referred to as highly oxidised organic molecules (HOMs) with low volatility. Such HOMs are formed through *autooxidation* reactions involving peroxy radicals: this process is detailed by Bianchi et al. (2019), and the subtle but important difference between HOMs and molecules with high oxygen content is laid out. Briefly, HOMs are species of very low vapour pressure so that condensation onto existing particles is very probable and almost irreversible (Bianchi et al., 2019). High yields of HOMs have been observed for isoprene and the monoterpenes α-pinene and especially limonene (Bianchi et al., 2019), with total yields of 4 % (isoprene), (7.0 ± 3.5)…(3.4 ± 1.0) % (α-pinene) and 17.0 ± 8.5 % (limonene), respectively (Bianchi et al., 2019; Jokinen et al., 2015; Ng et al., 2008; Ehn et al., 2014; Kirkby et al., 2016). It may therefore be assumed that derivatives — or more precisely oxidation products — of monoterpenes or isoprene are common in SOA. Building on the work of Saunders et al. (2012), chosing an oxidation product of isoprene or monoterpenes as the investigated organics may constitute a more realistc proxy for aerosol organics.

Recently, Reza et al. (2024) have performed similar experiments as Saunders et al. (2012), but using organic species better representing VOC oxidation. Recent observations have shown elevated concentrations of $IO^{\bullet}$ (g) in dust layers above the Atacama and Sechura deserts: Koenig, Volkamer, et al. (2021) measured a ten-fold enhancement of iodine monoxide radical concentrations compared to the regional background signal of 0.10…0.25 pptv. Because iron is hypothetised to catalyse photochemistry in dust particles, and since it is the most abundant transition metal in dust minerals (A. Al-Abadleh et al., 2023), iron may serve as a proxy for dust when investigating the reduction

of iodate. In a series of coated wall flow tube reactor (CWFTR) experiments, Reza et al. (2024) used a cavity-enhanced differential optical absorbtion spectroscopy (CE-DOAS) to detect I_2(g) and a ?? to detect OVOCs associated with iodate reduction in thin aqueous films. The films were inserted into the CWFTR and consisted of an organic or inorganic matrix and iodate. The organic matrices included iron(III)-citrate, citric acid (CA) and 1,2,3,4 butanetetracarboxylic acid (BTCA). CA was found in aerosol (Lienhard et al., 2012) and is a proxy for oxygenated organic species. Fe-Cit, as a known photoactive compound, is considered a suitable proxy for Fe(III) carboxylate complexes found in the atmosphere (Reza et al., 2024). Importantly, CA has well-characterised hygroscopic properties (Reza et al., 2024) so that this matrix can be used to control against matrix effects of organics that are due to iron when using Fe-Cit. These matrices were mixed with a solution of sodium iodate ($NaIO_3$) to introduce iodate at a concentration of ≈ 30 mM. The results show that irradiation with VIS for films containing Fe-Cit led to the reduction of $\approx 40\,\%$ of the initially present iodate. Likely, Fe-Cit undergoes a ligand-to-metal charge transfer (LMCT) induced through irradiance with a photon at $\lambda < 500$ nm to yield citrate (Cit) radicals and solvated electrons e^-(aq), as described by Saunders et al. (2012). Likely, reduction of iodate is driven through these solvated electrons. Furthermore, Reza et al. (2024) report that the speciation of the chromophores may include iodine-containing compounds.

5 Introduction

Iodine is the heaviest stable halogen element with atomic number 53. It has an average atomic weight of 126.904 u and forms a semi-lustrous solid under standard conditions (here 273.15 K and 1 bar, see Calvert (1990)) (Kaiho, 2015). Its melting and boiling points are 114 °C and 184 °C, respectively, and its vapour pressure is 0.031 kPa and 9.17 kPa at 25 °C and 113.6 °C, respectively (Kaiho, 2015). The atomic radius of iodine is 140 pm and its first ionisation energy is 1015 kJ mol^{-1} (Kaiho, 2015). Iodine is important in the enviornment: in the atmosphere, it influences the chemistry of ozone and important radical species, and it may be cause the formation of particles that may act as nuclei for aerosol or clouds (Saiz-Lopez, Plane, et al., 2012). The former is important for the capability of the atmophere to oxidise and remove species emitted to it, while the latter is important because of its effect on radiative equilibrium of Earth.

5.1 Iodine in the environment

Iodine is litophilic and incompatible in Earth's astenosphere, and therefore concentrated in oceans and surface sediments (Kendrick, 2024). Marine sediments constitute the largest iodine reservoir (Kendrick, 2024) with much higher concentrations of 20…600 mg kg^{-1} compared to soil- (0.5…20 mg kg^{-1}) or rock (0.08…0.5 mg kg^{-1}) concentrations (Whitehead, 1984). Sedimented iodine may be recycled into the oceans through sedimentary brines (Muramatsu, Fehn, et al., 2001; Muramatsu, Yoshida, et al., 2004) around techtonically active subduction zones (Carrano et al., 2020) through diagenesis processes involving thermal decompostion or microbiological reduction of buried organic matter (Kendrick, 2024; Muramatsu, Fehn, et al., 2001). Consequently, iodine concentrations in the oceans are approximately 45…60 µg L^{-1} (Whitehead, 1984), mostly in the form of iodate, the thermodynamically most stable state of iodine in aqueous solution (Fuge et al., 2015). However, iodate exhibits a nutrient-like profile (Carrano et al., 2020) being depleted at the surface, whereas iodide is enriched in the surface (Elderfield et al., 1980). Similarly, organic matter is enriched in the surface, so that the existence of some iodinated organics may be presumed (Saiz-Lopez, Plane, et al., 2012). Within the oceans, iodine is incorporated preferrentially in organic matter (Kendrick, 2024) by micro- and macroalgae, and aerobic bacteria (L. Carpenter, 2015): through faciliated diffusion (see detailed descriptions in Küpper et al. (2008), Winter et al. (2009), and Amachi (2008)), cells store iodine as I^-(aq) or associated to organic molecules (Küpper et al., 2008; Amachi, 2008). Iodide within the cell interior may act as an antioxidant (Küpper et al., 2008): upon oxidative stress, the iodide reservoir is mobilised and cells emit I^-(aq) and a range of VOICs (Küpper et al., 2008; L. Carpenter, 2015) that may volatilise to the atmosphere. Analogously, when oxidative stress occurs during air exposure at low tide, the hetergeneous surface reaction of iodide and ozone at the sea-water interface produces hypoiodous acid, molecular iodine and iodine monoxide radicals directly emitted to the atmosphere (L. Carpenter, 2015; Palmer et al., 2005; Liu et al., 2001; Sakamoto et al., 2009; Hayase et al., 2010; He et al., 2021). It is currently thought that the biggest source of inorganic iodine to the atmosphere is hypoiodous acid produced via the same pathway, exceeding the emissions of molecular iodine by one order of magnitude (L. J. Carpenter et al., 2013). Nevertheless, the atmospheric iodine budget is currently not well-constrained (Saiz-Lopez, Plane, et al., 2012). VOICs (notably CH_3I) and inorganic iodine species (HOI, I_2, $IO^\bullet$) emitted from the oceans constitute the biggest source of iodine to the atmosphere (L. Carpenter, 2015; L. J. Carpenter et al., 2013), with estimated input $\approx$ 550 Gg yr^{-1} (Saiz-Lopez, Plane, et al., 2012). Most VOICs are photolabile with lifetimes on the order of minutes to days (Bloss et al., 2001). Other natural sources of iodine to the amtosphere include soils and plants (Whitehead,

1984; L. Carpenter, 2015; Fuge et al., 2015), terrestrial water systems (Whitehead, 1984), and volcanoes or salt lakes (L. Carpenter, 2015). The additional input from terrestrial sources into the atmosphere is $\approx 80 \ldots 110\,\mathrm{Gg\,yr^{-1}}$ (Saiz-Lopez, Plane, et al., 2012). Anthropogenic sources include direct emissions from fossil fuel burning (Fuge et al., 2015) and pesticide use (Zheng et al., 2003; Whitehead, 1984). There are indirect anthropogenic effects as well: ice core data indicates that the sea-air flux of iodine has tripled between 1950 and 2010 as a consequence of increased anthropogenic ozone pollution of the troposphere (Cuevas et al., 2018). Sinks of atmospheric iodine include wet- and dry deposition (Fuge et al., 2015), and direct uptake through plants (Fuge et al., 2015). Overall, this leads to boundary layer mixing ratios of $\chi_{\mathrm{I_2(g)}} \leq 93\,\mathrm{pptv}$ (L. Carpenter, 2015), $\chi_{\mathrm{IO^{\bullet}(g)}} \leq 3 \ldots 20\,\mathrm{pptv}$ (L. Carpenter, 2015), $\chi_{\mathrm{HOI(g)}} \leq 1\,\mathrm{pptv}$ (He et al., 2021) and $\chi_{\mathrm{I^{\bullet}(g)}} \leq 0.1 \ldots 22\,\mathrm{pptv}$ (L. Carpenter, 2015; He et al., 2021).

5.2 Iodine Chemistry in the Atmosphere

The importance of the marine iodine source is likely also reflected in aerosol composition: above marine areas, aerosol is enriched in iodine relative to seawater content by a factor of 100…1000 (L. Carpenter, 2015). Iodine may be transported into the aerosol phase through bubble-bursting of iodine-rich surface ocean waters (Saiz-Lopez, Plane, et al., 2012), or through the formation of aerosol via IOPs (O'Dowd et al., 2002). Likely, low-volatility iodinated organics may also condense into the aerosol phase. Overall, various iodinated species may be present in aerosol including iodide, iodate, hypoiodous acid and SOI (Saiz-Lopez, Plane, et al., 2012). Saiz-Lopez, Plane, et al. (2012) and Gilfedder et al. (2008) report that SOI is very frequent in aerosol and may constitute the largest reservoir of iodine in aerosol. There appear to be two principal pathways of SOI accomodation: direct accumulation from sea spray enriched in iodinated organics, and the reaction of hypoiodous acid with aerosol organics. Hypoiodous acid may also be highly reactive towards other species, likely due to its affinity for nucelophilic attacks on susceptible species. In general however, hypoiodous acid or other likewise reduced iodine species such as iodide should be oxidised to iodate (Gilfedder et al., 2008), the thermodynamically most stable form of iodine in aqueous solution. Consequently, the accumulated form of iodine in condensed aerosol phases is often thought to be iodate (Gilfedder et al., 2008; Saiz-Lopez, Plane, et al., 2012). However, observations in the troposphere indicate higher aerosol contents of iodide than iodate (Gilfedder et al., 2008), or high variability in the iodide/iodate ratio (Saiz-Lopez, Plane, et al., 2012). This indicates the presence of a mechanism reducing iodate in the troposphere.

Hetergeneous aerosol chemistry of iodine is closely linked to homogeneous chemistry of iodine through many iodine species. Generally, atmospheric iodine chemistry is initiated mostly through RIS such as iodine radicals or iodine monoxide radicals. Briefly, homogeneous iodine chemistry involves catalytic destruction of troposheric ozone via various pathways involving hydrogen oxide radicals (HO_x) and nitrous oxides as well as other halogen atoms in the atmosphere (Saiz-Lopez and Von Glasow, 2012). This process is photochemically driven and initiated with $\mathrm{IO^{\bullet}}$ and $\mathrm{I^{\bullet}}$. Saiz-Lopez and Von Glasow (2012) have outlined the mechanism: the intial step is the production of iodine radicals from VOICs or molecular iodine. The iodine radicals react with ozone to produce iodine monoxide radicals that in turn recombine to again produce iodine radicals:

$$\mathrm{RI(g)} + h\nu \longrightarrow \mathrm{R^{\bullet}(g)} + \mathrm{I^{\bullet}(g)} \qquad \text{[R5.2.1]}$$

$$\mathrm{I_2(g)} + h\nu \longrightarrow 2\,\mathrm{I^{\bullet}(g)} \qquad \text{[R5.2.2]}$$

$$\mathrm{I^{\bullet}(g)} + \mathrm{O_3(g)} \longrightarrow \mathrm{IO^{\bullet}(g)} + \mathrm{O_2(g)} \qquad \text{[R5.2.3]}$$

$$2\,\mathrm{IO^{\bullet}} \longrightarrow 2\,\mathrm{I^{\bullet}(g)} + \mathrm{O_2(g)} \qquad \text{[R5.2.4]}$$

The net outcome is ozone destruction with $2\,\mathrm{O_3(g)} \longrightarrow 3\,\mathrm{O_2(g)}$, although reaction 5.2.4 has other channels that may involve HO_x and

NO_x cycles. Importantly, the iodine monoxide radical has a lifetime against photolysis in the boundary layer on the order of seconds (Bloss et al., 2001). Likewise, the effective lifetime of iodine radical species against uptake in aerosol is on the order of hours (Dix et al., 2013): sustained presence of iodine monoxide radicals in the atmosphere therefore requires an effective recycling mechanism for $IO^{\bullet}$.
Additionally, iodine may be involved in the oxidation of atmospheric organic molecules or mercury, allowing the latter to enter the food chain as highly poisonous methylmercury (Steffen et al., 2008; Saiz-Lopez and Von Glasow, 2012; Saiz-Lopez, Plane, et al., 2012), and likely leading to enhanced condensation of organics into the aerosol phase through the former. Further, through formation of IOPs, iodine oxides may lead to the production of UFAPs (L. Carpenter, 2015). Volatile species may condense on UFAPs that can grow up to the point of becoming CNNs (Saiz-Lopez, Plane, et al., 2012). Recent evidence shows that nucleation via iodine oxoacids to produce IOPs is highly efficient and sometimes competitive with sulfuric acid-ammonium driven nucleation (He et al., 2021). Moreover, heterogeneous iodine chemistry on pre-existing frozen or liquid salt particles may lead to sudden increases in gas phase iodine species (Saiz-Lopez and Von Glasow, 2012). Importantly, the reaction of bromide with ozone on frozen salt solutions occurs in the brine pertaining to the bulk ice phase, rather than *within* the bulk ice phase (Oldridge et al., 2011): such brines are formed when freezing solutions exclude solutes — the heterogeneous reaction of ozone with iodide on frozen aerosol is here assumed to behave similarly. In other words, the heterogeneous reaction of ozone with aerosol surfaces is assumed to be similar for frozen and liquid aerosol particles.
Other heterogeneous effects may lead to substantial iodine emissions through the reaction of ozone with dissolved iodide in ocean and aerosols (Palmer et al., 2005; Liu et al., 2001; Sakamoto et al., 2009; Hayase et al., 2010). In the upper troposphere and lower stratosphere, heterogeneous recycling of iodine species is highly important: Model calculations by Saiz-Lopez, Baidar, et al. (2015) show that from the lower troposphere, convection may transport inorganic- and organic iodine species to the lower stratosphere, causing a total inorganic iodine injection of 0.25…0.7 pptv (Saiz-Lopez, Baidar, et al., 2015). Measurements by Koenig, Baidar, et al. (2020) are in agreement with this, indicating an injection of 0.77 ± 0.10 pptv of I_y into the lower stratosphere. Associated therewith is a mixing ratio of $\chi_{IO^{\bullet}(g)} = 0.06 \pm 0.03$ pptv even for aged stratospheric air. Koenig, Baidar, et al. (2020) also observed that increases in altitude across the troposphere are associated with (1) an increase in particulate iodine and a decrease in gas phase iodine; and (2) a shift of iodide-iodate speciation in the condensed phase towards iodate. Simulations could reproduce observed $\chi_{IO^{\bullet}(g)}$ only when a recycling scheme for iodine on ice particles was applied, and when the proper partioning between condensed- and gas phase was applied. This indicates that, as for the troposphere, a recycling mechanism producing gas phase iodine monoxide radicals must exist. There is also evidence that iodate should be reduced to iodide: Pillar-Little et al. (2013) have established a pathway through which iodide and ozone cause volatilization of I_2(g) and HOI(g) from watery microdroplets. However, it is still unclear *how* the necessary iodide is formed, given that most iodine should be present as iodate. Consequently, an important question to answer is: how is IO_3^- reduced to species — most likely I^- — that may, directly of after reacting, volatilise to the gas phase?

5.3 Reduction of Iodate

Saunders et al. (2012) have shown that iodate may be reduced when solutions of iodate and HA are irradiated with UV-A and VIS light between $\lambda \geq 310$ nm and $\lambda \approx 780$ nm. The light source was filtered to exclude IR light and lamp output below $\lambda = 310$ nm to simulate the UV-A-VIS solar spectrum in the lower troposphere. They found that the major product of this photochemically induced process was SOI and that the proportion of iodide in the reactant solution remained constant at approximately 20 %. Since HA is a chromophore, the suggested mechanism involves photogeneration of solvated electrons e^-(aq) that, in dependence of pH, yield hypoiodous acid: $IO_3^-(aq) + 4\,e^-(aq) + 5\,H^+(aq) \longrightarrow HOI(aq) + 2\,H_2O(aq)$. From there, SOI may be created through the nucleophilic attack of hypoiodous acid on diphenolic functional groups (Saunders et al., 2012). Alternatively, molecular iodine may be produced through reaction 5.3.1, as described by Pillar-Little et al. (2013):

$$HOI(aq) + I^- + H^+(aq) \longrightarrow I_2(aq) + H_2O(l) \quad [R5.3.1]$$

Since molecular iodine is insoluble (Saiz-Lopez, Plane, et al., 2012), there will be volatilisation of molecular iodine to the gas phase. Overall, the mechanism suggested by Saunders et al. (2012) produces primarily hypoiodous acid molecular iodine — the production pathway of iodide has not been elucidated. The presence of iodide, however, appears necessary for the production of I_2(g). It is hypothetised that iodide may be regenerated from SOI (Saunders et al., 2012; Baker, 2005). Finally, Saunders et al. (2012) have reported oscillations in the release of I_2(g). This is likely associated with formation of hydrogen peroxide as a byproduct of HA photolysis (Saunders et al., 2012). Indeed, Cooper et al. (1988) have shown that hydrogen peroxide is a common product when irradiating aqueous solutions of chromophores. Given hydrogen peroxide, oscillations in I_2-IO_3^- are known as the BLM, first described by Bray (1921) and Bray and Liebhafsky (1931): hydrogen peroxide interacts with molecular iodine and iodate via

$$2\,IO_3^-(aq) + 2\,H^+(aq) + 5\,H_2O_2(aq) \rightleftharpoons I_2(aq) + 5\,O_2(g) + 6\,H_2O(l) \quad [R5.3.2]$$

$$I_2(aq) + 5\,H_2O_2(aq) \rightleftharpoons 2\,IO_3^-(aq) + 2\,H^+(aq) + 4\,H_2O(l) \quad [R5.3.3]$$

to yield a net catalytic decomposition of hydrogen peroxide via

$$2\,H_2O_2(aq) \longrightarrow 2\,H_2O(l) + O_2(g) \quad [R5.3.4]$$

The oscillation reaction has a *stable* regime — here, all species reach steady state except H_2O_2: likely, O_2(g) volatilises and LCP dictates that hydrogen peroxide consequently depletes. The *unstable* regime where either reaction 5.3.2 or 5.3.3 occur preferrentially, leads to oscillations in molecular iodine and iodate. These oscillations are modulated by initial pH (Bray, 1921) and temperature. Including an organic reducing agent and a metal-ion catalyst results in the BRM after Briggs et al. (1973), elucidated by Schmitz et al. (2012): Briefly, in addition to reaction 5.3.3, the presence of some organic species $R-H_2$ will induce the following reactions:

$$H^+(aq) + IO_3^-(aq) + 2\,I_2(aq) + 5\,R{-}H_2(aq) \longrightarrow 5\,R{-}HI + 3\,H_2O \quad [R5.3.5]$$

$$H^+(aq) + IO_3^-(aq) + 2\,I_2(aq) + 5\,R{-}HI(aq) \longrightarrow 5\,R{-}I_2 + 3\,H_2O \quad [R5.3.6]$$

$$R{-}I_2 + R{-}H_2 \rightleftharpoons 2\,R{-}HI \quad [R5.3.7]$$

The backward reaction likely proceeds via the metal ion catalyst, although Schmitz et al. (2012) reported the possibility of non-catalysed pathways.

A lot has been learned so far: organic substances may lead to the reduction of iodate, via chromophore activity. Furthermore, observed oscillations in gas phase I_2 may be explained through BLM-BRM mechanisms. However, the suitability of HAs to represent organic aerosol has been questioned: Graber et al. (2006) suggested that humic-like substances found in aerosol particles may differ substantially from humic substances found in soil. More specifically, Graber et al. (2006) argue that terrestrial sources — from which the HA used by Saunders et al. (2012) likely originate — may not be the origin of the majority of humic-like substances in aerosol. Differences may be found in terms of molecular weight, aromatic moiety content, surface properties and other properties (Graber et al., 2006). Although

HAs as organics have profen useful to elucidate the mechanisms of I_2 recycling, quantitatively constraining this recycling better requires more realistic organics. Another important question to answer, therefore, is: are there proxies that represent organics in aerosol more accurately, and to which the same chromophore-dependent pathway of iodine recycling applies?

5.4 Reduction of Iodate: Proxies for Secondary Organic Aerosol

A. Guenther et al. (1995) modelled global natural VOC emissions in 1990. They found a total flux of 1150 TgC yr^{-1}, of which 44 % (503 TgC yr^{-1}) was isoprene and 11 % (127 TgC yr^{-1}) were monoterpenes such as α-pinene. Thereof, approximately 75 % orginated from forests. In 2006, The annual atmospheric VOC injection was further specified in 2012 when A. B. Guenther et al. (2012) reported the following emissions of VOCs for the year 2000: total emissions were 1089 TgC yr^{-1}, of which isoprene emissions were 49.1 % (535 TgC yr^{-1}) and the monoterpenes α-pinene, β-pinene and limonene contributed 6.7 % (66.1 TgC yr^{-1}), 1.7 % (18.9 TgC yr^{-1}) and 1.0 % (11.4 TgC yr^{-1}), respectively. isoprene and monoterpene emissions are biogenic and mostly linked to vegetation — overall they contributed approximately 65 % to global VOC emissions in 2000 (A. B. Guenther et al., 2012), rendering them a major source of atmospheric VOCs.

Organic matter in aerosol is present either as POA or SOA. POA and SOA comprise the largest share of *fine* particles with diameters $d \leq 2.5\,\mu m$. On the other hand, large particles with diameters $d > 2.5\,\mu m$ are mostly comprised of particles formed mechanically, including soil and mineral dust, sea salt particles and plant particles (J. Ziemann et al., 2012). POA requires no chemical reactions to condense to the aerosol phase. Conversely, SOA is created when volatile precursor species are chemically altered to lower volatilities, and consequently condense to the aerosol phase. Likely, SOA constitues a large fraction of organic aerosol Bianchi et al., 2019; Hallquist et al., 2009. As a general rule of thumb, higher oxygen content of a molecule indicates *lower* volatility. Therefore, oxidation reactions are highly important in SOA formation because oxidation effectively *decreases* volatility. Recent work summarised by Bianchi et al. (2019) suggests that there exists class of of low-volatile species referred to as HOMs with low volatility. Such HOMs are formed through *autooxidation* reactions involving peroxy radicals: this process is detailed by Bianchi et al. (2019), and the subtle but important difference between HOMs and molecules with high oxygen content is laid out. Briefly, HOMs are species of very low vapour pressure so that condensation onto existing particles is very probable and almost irreversible (Bianchi et al., 2019). High yields of HOMs have been observed for isoprene and the monoterpenes α-pinene and especially limonene (Bianchi et al., 2019), with total yields of 4 % (isoprene), (7.0 ± 3.5)…(3.4 ± 1.0) % (α-pinene) and 17.0 ± 8.5 % (limonene), respectively (Bianchi et al., 2019; Jokinen et al., 2015; Ng et al., 2008; Ehn et al., 2014; Kirkby et al., 2016). It may therefore be assumed that derivatives — or more precisely oxidation products — of monoterpenes or isoprene are common in SOA. Building on the work of Saunders et al. (2012), chosing an oxidation product of isoprene or monoterpenes as the investigated organics may constitute a more realistc proxy for aerosol organics.

Recently, Reza et al. (2024) have performed similar experiments as Saunders et al. (2012), but using organic species better representing VOC oxidation. Recent observations have shown elevated concentrations of $IO^{\bullet}$ (g) in dust layers above the Atacama and Sechura deserts: Koenig, Volkamer, et al. (2021) measured a ten-fold enhancement of iodine monoxide radical concentrations compared to the regional background signal of 0.10…0.25 pptv. Because iron is hypothetised to catalyse photochemistry in dust particles, and since it is the most abundant transition metal in dust minerals (A. Al-Abadleh et al., 2023), iron may serve as a proxy for dust when investigating the reduction of iodate. In a series of CWFTR experiments, Reza et al. (2024) used a CE-DOAS to detect I_2(g) and a ?? to detect OVOCs associated with iodate reduction in thin aqueous films. The films were inserted into the CWFTR and consisted of an organic or inorganic matrix and iodate. The organic matrices included Fe-Cit, CA and BTCA. CA was found in aerosol (Lienhard et al., 2012) and is a proxy for oxygenated organic species. Fe-Cit, as a known photoactive compound, is considered a suitable proxy for Fe(III) carboxylate complexes found in the atmosphere (Reza et al., 2024). Importantly, CA has well-characterised hygroscopic properties (Reza et al., 2024) so that this matrix can be used to control against matrix effects of organics that are due to iron when using Fe-Cit. These matrices were mixed with a solution of

sodium iodate to introduce iodate at a concentration of $\approx$ 30 mM. The results show that irradiation with VIS for films containing Fe-Cit led to the reduction of $\approx$ 40 % of the initially present iodate. Likely, Fe-Cit undergoes a LMCT induced through irradiance with a photon at $\lambda < 500$ nm to yield Cit radicals and solvated electrons e^-(aq), as described by Saunders et al. (2012). Likely, reduction of iodate is driven through these solvated electrons. Furthermore, Reza et al. (2024) report that the speciation of the chromophores may include iodine-containing compounds.

6 Acknowledgements

Dr. David Bell, Laso Blabla, Dominik Blabla, Wei Huang, Thorsten Bartels-Rausch, Marco Paolini, Yiwei Gong, Sacha Fallah, Francesca Salteri,

Bibliography

A. Al-Abadleh, H., J. D. Kubicki, and N. Meskhidze (2023). "A perspective on iron (Fe) in the atmosphere: air quality, climate, and the ocean". In: *Environmental Science: Processes & Impacts* 25.2, pp. 151–164.

Amachi, S. (2008). "Microbial contribution to global iodine cycling: Volatilization, accumulation, reduction, oxidation, and sorption of iodine". In: *Microbes and Environments* 23.4, pp. 269–276.

Baker, A. R. (Dec. 8, 2005). "Marine Aerosol Iodine Chemistry: The Importance of Soluble Organic Iodine". In: *Environmental Chemistry* 2.4, pp. 295–298.

Bianchi, F., T. Kurtén, M. Riva, C. Mohr, M. P. Rissanen, P. Roldin, T. Berndt, J. D. Crounse, P. O. Wennberg, T. F. Mentel, J. Wildt, H. Junninen, T. Jokinen, M. Kulmala, D. R. Worsnop, J. A. Thornton, N. Donahue, H. G. Kjaergaard, and M. Ehn (Mar. 27, 2019). "Highly Oxygenated Organic Molecules (HOM) from Gas-Phase Autoxidation Involving Peroxy Radicals: A Key Contributor to Atmospheric Aerosol". In: *Chemical Reviews* 119.6, pp. 3472–3509.

Bloss, W. J., D. M. Rowley, R. A. Cox, and R. L. Jones (Aug. 1, 2001). "Kinetics and Products of the IO Self-Reaction". In: *The Journal of Physical Chemistry A* 105.33, pp. 7840–7854.

Bray, W. C. (June 1, 1921). "A periodic reaction in homogeneous solution and its relation to catalysis". In: *Journal of the American Chemical Society* 43.6, pp. 1262–1267.

Bray, W. C. and H. A. Liebhafsky (Jan. 1, 1931). "Reactions involving hydrogen peroxide, iodine and iodate ion". In: *Journal of the American Chemical Society* 53.1, pp. 38–44.

Briggs, T. S. and W. C. Rauscher (July 1, 1973). "An oscillating iodine clock". In: *Journal of Chemical Education* 50.7, p. 496.

Calvert, J. G. (Jan. 1, 1990). "Glossary of atmospheric chemistry terms (Recommendations 1990)". In: *Pure and Applied Chemistry* 62.11, pp. 2167–2219.

Carpenter, L. (2015). "Biogeochemical Cycles - Iodine". In: *Encyclopedia of Atmospheric Sciences*. 2nd ed. Elsevier, pp. 205–219.

Carpenter, L. J., S. M. MacDonald, M. D. Shaw, R. Kumar, R. W. Saunders, R. Parthipan, J. Wilson, and J. M. C. Plane (Feb. 2013). "Atmospheric iodine levels influenced by sea surface emissions of inorganic iodine". In: *Nature Geoscience* 6.2, pp. 108–111.

Carrano, M. W., K. Yarimizu, J. L. Gonzales, R. Cruz-López, M. S. Edwards, T. M. Tymon, F. C. Küpper, C. J. Carrano, M. W. Carrano, K. Yarimizu, J. L. Gonzales, R. Cruz-López, M. S. Edwards, T. M. Tymon, F. C. Küpper, and C. J. Carrano (June 15, 2020). "The influence of marine algae on iodine speciation in the coastal ocean". In: *Algae* 35.2, pp. 167–176.

Cooper, W. J., R. G. Zika, R. G. Petasne, and J. M. C. Plane (Oct. 1, 1988). "Photochemical formation of hydrogen peroxide in natural waters exposed to sunlight". In: *Environmental Science & Technology* 22.10, pp. 1156–1160.

Cuevas, C. A., N. Maffezzoli, J. P. Corella, A. Spolaor, P. Vallelonga, H. A. Kjær, M. Simonsen, M. Winstrup, B. Vinther, C. Horvat, R. P. Fernandez, D. Kinnison, J.-F. Lamarque, C. Barbante, and A. Saiz-Lopez (Apr. 13, 2018). "Rapid increase in atmospheric iodine levels in the North Atlantic since the mid-20th century". In: *Nature Communications* 9.1, p. 1452.

Dix, B., S. Baidar, J. F. Bresch, S. R. Hall, K. S. Schmidt, S. Wang, and R. Volkamer (Feb. 5, 2013). "Detection of iodine monoxide in the tropical free troposphere". In: *Proceedings of the National Academy of Sciences* 110.6, pp. 2035–2040.

Ehn, M., J. A. Thornton, E. Kleist, M. Sipilä, H. Junninen, I. Pullinen, M. Springer, F. Rubach, R. Tillmann, B. Lee, F. Lopez-Hilfiker, S. Andres, I.-H. Acir, M. Rissanen, T. Jokinen, S. Schobesberger, J. Kangasluoma, J. Kontkanen, T. Nieminen, T. Kurtén, L. B. Nielsen, S. Jørgensen, H. G. Kjaergaard, M. Canagaratna, M. D. Maso, T. Berndt, T. Petäjä, A. Wahner, V.-M. Kerminen, M. Kulmala, D. R. Worsnop, J. Wildt, and T. F. Mentel (Feb. 2014). "A large source of low-volatility secondary organic aerosol". In: *Nature* 506.7489, pp. 476–479.

Elderfield, H. and V. W. Truesdale (Oct. 1, 1980). "On the biophilic nature of iodine in seawater". In: *Earth and Planetary Science Letters* 50.1, pp. 105–114.

Fuge, R. and C. C. Johnson (Dec. 1, 2015). "Iodine and human health, the role of environmental geochemistry and diet, a review". In: *Applied Geochemistry* 63, pp. 282–302.

Gilfedder, B. S., S. C. Lai, M. Petri, H. Biester, and T. Hoffmann (Oct. 21, 2008). "Iodine speciation in rain, snow and aerosols". In: *Atmospheric Chemistry and Physics* 8.20, pp. 6069–6084.

Graber, E. R. and Y. Rudich (Mar. 6, 2006). "Atmospheric HULIS: How humic-like are they? A comprehensive and critical review". In: *Atmospheric Chemistry and Physics* 6.3, pp. 729–753.

Guenther, A. B., X. Jiang, C. L. Heald, T. Sakulyanontvittaya, T. Duhl, L. K. Emmons, and X. Wang (Nov. 26, 2012). "The Model of Emissions of Gases and Aerosols from Nature version 2.1 (MEGAN2.1): an extended and updated framework for modeling biogenic emissions". In: *Geoscientific Model Development* 5.6, pp. 1471–1492.

Guenther, A., C. N. Hewitt, D. Erickson, R. Fall, C. Geron, T. Graedel, P. Harley, L. Klinger, M. Lerdau, W. A. Mckay, T. Pierce, B. Scholes, R. Steinbrecher, R. Tallamraju, J. Taylor, and P. Zimmerman (1995). "A global model of natural volatile organic compound emissions". In: *Journal of Geophysical Research: Atmospheres* 100 (D5), pp. 8873–8892.

Hallquist, M., J. C. Wenger, U. Baltensperger, Y. Rudich, D. Simpson, M. Claeys, J. Dommen, N. M. Donahue, C. George, A. H. Goldstein, J. F. Hamilton, H. Herrmann, T. Hoffmann, Y. Iinuma, M. Jang, M. E. Jenkin, J. L. Jimenez, A. Kiendler-Scharr, W. Maenhaut, G. McFiggans, T. F. Mentel, A. Monod, A. S. H. Prévôt, J. H. Seinfeld, J. D. Surratt, R. Szmigielski, and J. Wildt (July 29, 2009). "The formation, properties and impact of secondary organic aerosol: current and emerging issues". In: *Atmospheric Chemistry and Physics* 9.14, pp. 5155–5236.

Hayase, S., A. Yabushita, M. Kawasaki, S. Enami, M. R. Hoffmann, and A. J. Colussi (May 20, 2010). "Heterogeneous Reaction of Gaseous Ozone with Aqueous Iodide in the Presence of Aqueous Organic Species". In: *The Journal of Physical Chemistry A* 114.19, pp. 6016–6021.

He, X.-C. et al. (Feb. 5, 2021). "Role of iodine oxoacids in atmospheric aerosol nucleation". In: *Science* 371.6529, pp. 589–595.

J. Ziemann, P. and R. Atkinson (2012). "Kinetics, products, and mechanisms of secondary organic aerosol formation". In: *Chemical Society Reviews* 41.19, pp. 6582–6605.

Jokinen, T., T. Berndt, R. Makkonen, V.-M. Kerminen, H. Junninen, P. Paasonen, F. Stratmann, H. Herrmann, A. B. Guenther, D. R. Worsnop, M. Kulmala, M. Ehn, and M. Sipilä (June 9, 2015). "Production of extremely low volatile organic compounds from biogenic emissions: Measured yields and atmospheric implications". In: *Proceedings of the National Academy of Sciences* 112.23, pp. 7123–7128.

Kaiho, T. (2015). "Physical Properties of Iodine". In: *Iodine Chemistry and Applications*. Hoboken: John Wiley & Sons, pp. 7–14.

Kendrick, M. A. (July 23, 2024). "Halogen Cycling in the Solid Earth". In: *Annual Review of Earth and Planetary Sciences* 52 (Volume 52, 2024), pp. 195–220.

Kirkby, J., J. Duplissy, K. Sengupta, C. Frege, H. Gordon, C. Williamson, M. Heinritzi, M. Simon, C. Yan, J. Almeida, J. Tröstl, T. Nieminen, I. K. Ortega, R. Wagner, A. Adamov, A. Amorim, A.-K. Bernhammer, F. Bianchi, M. Breitenlechner, S. Brilke, X. Chen, J. Craven, A. Dias, S. Ehrhart, R. C. Flagan, A. Franchin, C. Fuchs, R. Guida, J. Hakala, C. R. Hoyle, T. Jokinen, H. Junninen, J. Kangasluoma, J. Kim, M. Krapf, A. Kürten, A. Laaksonen, K. Lehtipalo, V. Makhmutov, S. Mathot, U. Molteni, A. Onnela, O. Peräkylä, F. Piel, T. Petäjä, A. P. Praplan, K. Pringle, A. Rap, N. A. D. Richards, I. Riipinen, M. P. Rissanen, L. Rondo, N. Sarnela, S. Schobesberger, C. E. Scott, J. H. Seinfeld, M. Sipilä, G. Steiner, Y. Stozhkov, F. Stratmann, A. Tomé, A. Virtanen, A. L. Vogel, A. C. Wagner, P. E. Wagner, E. Weingartner, D. Wimmer, P. M. Winkler, P. Ye, X. Zhang, A. Hansel, J. Dommen, N. M. Donahue, D. R. Worsnop, U. Baltensperger, M. Kulmala, K. S. Carslaw, and J. Curtius (May 2016). "Ion-induced nucleation of pure biogenic particles". In: *Nature* 533.7604, pp. 521–526.

Koenig, T. K., S. Baidar, P. Campuzano-Jost, C. A. Cuevas, B. Dix, R. P. Fernandez, H. Guo, S. R. Hall, D. Kinnison, B. A. Nault, K. Ullmann, J. L. Jimenez, A. Saiz-Lopez, and R. Volkamer (Jan. 28, 2020). "Quantitative detection of iodine in the stratosphere". In: *Proceedings of the National Academy of Sciences* 117.4, pp. 1860–1866.

Koenig, T. K., R. Volkamer, E. C. Apel, J. F. Bresch, C. A. Cuevas, B. Dix, E. W. Eloranta, R. P. Fernandez, S. R. Hall, R. S. Hornbrook, R. B. Pierce, J. M. Reeves, A. Saiz-Lopez, and K. Ullmann (Dec. 22, 2021). "Ozone depletion due to dust release of iodine in the free troposphere". In: *Science Advances* 7.52, eabj6544.

Küpper, F. C., L. J. Carpenter, G. B. McFiggans, C. J. Palmer, T. J. Waite, E.-M. Boneberg, S. Woitsch, M. Weiller, R. Abela, D. Grolimund, P. Potin, A. Butler, G. W. Luther, P. M. H. Kroneck, W. Meyer-Klaucke, and M. C. Feiters (May 13, 2008). "Iodide accumulation provides kelp with an inorganic antioxidant impacting atmospheric chemistry". In: *Proceedings of the National Academy of Sciences* 105.19, pp. 6954–6958.

Lienhard, D. M., D. L. Bones, A. Zuend, U. K. Krieger, J. P. Reid, and T. Peter (Oct. 11, 2012). "Measurements of Thermodynamic and Optical Properties of Selected Aqueous Organic and Organic–Inorganic Mixtures of Atmospheric Relevance". In: *The Journal of Physical Chemistry A* 116.40, pp. 9954–9968.

Liu, Q., L. M. Schurter, C. E. Muller, S. Aloisio, J. S. Francisco, and D. W. Margerum (Aug. 1, 2001). "Kinetics and Mechanisms of Aqueous Ozone Reactions with Bromide, Sulfite, Hydrogen Sulfite, Iodide, and Nitrite Ions". In: *Inorganic Chemistry* 40.17, pp. 4436–4442.

Messina, P., J. Lathière, K. Sindelarova, N. Vuichard, C. Granier, J. Ghattas, A. Cozic, and D. A. Hauglustaine (Nov. 16, 2016). "Global biogenic volatile organic compound emissions in the ORCHIDEE and MEGAN models and sensitivity to key parameters". In: *Atmospheric Chemistry and Physics* 16.22, pp. 14169–14202.

Muramatsu, Y., U. Fehn, and S. Yoshida (Nov. 15, 2001). "Recycling of iodine in fore-arc areas: evidence from the iodine brines in Chiba, Japan". In: *Earth and Planetary Science Letters* 192.4, pp. 583–593.

Muramatsu, Y., S. Yoshida, U. Fehn, S. Amachi, and Y. Ohmomo (Jan. 1, 2004). "Studies with natural and anthropogenic iodine isotopes: iodine distribution and cycling in the global environment". In: *Journal of Environmental Radioactivity*. Papers from the International Conference on Radioactivity in the Environment, Monaco, 1-5 September 2002 74.1, pp. 221–232.

Ng, N. L., A. J. Kwan, J. D. Surratt, A. W. H. Chan, P. S. Chhabra, A. Sorooshian, H. O. T. Pye, J. D. Crounse, P. O. Wennberg, R. C. Flagan, and J. H. Seinfeld (Aug. 1, 2008). "Secondary organic aerosol (SOA) formation from reaction of isoprene with nitrate radicals (NO_3)". In: *Atmospheric Chemistry and Physics* 8.14, pp. 4117–4140.

O'Dowd, C. D., J. L. Jimenez, R. Bahreini, R. C. Flagan, J. H. Seinfeld, K. Hämeri, L. Pirjola, M. Kulmala, S. G. Jennings, and T. Hoffmann (June 2002). "Marine aerosol formation from biogenic iodine emissions". In: *Nature* 417.6889, pp. 632–636.

Oldridge, N. W. and J. P. D. Abbatt (Mar. 31, 2011). "Formation of Gas-Phase Bromine from Interaction of Ozone with Frozen and Liquid NaCl/NaBr Solutions: Quantitative Separation of Surficial Chemistry from Bulk-Phase Reaction". In: *The Journal of Physical Chemistry A* 115.12, pp. 2590–2598.

Palmer, C. J., T. L. Anders, L. J. Carpenter, F. C. Küpper, and G. B. McFiggans (Dec. 8, 2005). "Iodine and Halocarbon Response of Laminaria digitata to Oxidative Stress and Links to Atmospheric New Particle Production". In: *Environmental Chemistry* 2.4, pp. 282–290.

Pillar-Little, E. A., M. I. Guzman, and J. M. Rodriguez (Oct. 1, 2013). "Conversion of Iodide to Hypoiodous Acid and Iodine in Aqueous Microdroplets Exposed to Ozone". In: *Environmental Science & Technology* 47.19, pp. 10971–10979.

Reza, M., L. Iezzi, H. Finkenzeller, A. Roose, M. Ammann, and R. Volkamer (Dec. 19, 2024). "Iodine Activation from Iodate Reduction in Aqueous Films via Photocatalyzed and Dark Reactions". In: *ACS Earth and Space Chemistry* 8.12, pp. 2495–2508.

Saiz-Lopez, A., S. Baidar, C. A. Cuevas, T. K. Koenig, R. P. Fernandez, B. Dix, D. E. Kinnison, J.-F. Lamarque, X. Rodriguez-Lloveras, T. L. Campos, and R. Volkamer (2015). "Injection of iodine to the stratosphere". In: *Geophysical Research Letters* 42.16, pp. 6852–6859.

Saiz-Lopez, A., J. M. C. Plane, A. R. Baker, L. J. Carpenter, R. Von Glasow, J. C. Gómez Martín, G. McFiggans, and R. W. Saunders (Mar. 14, 2012). "Atmospheric Chemistry of Iodine". In: *Chemical Reviews* 112.3, pp. 1773–1804.

Saiz-Lopez, A. and R. Von Glasow (2012). "Reactive halogen chemistry in the troposphere". In: *Chemical Society Reviews* 41.19, p. 6448.

Sakamoto, Y., A. Yabushita, M. Kawasaki, and S. Enami (July 9, 2009). "Direct Emission of I2 Molecule and IO Radical from the Heterogeneous Reactions of Gaseous Ozone with Aqueous Potassium Iodide Solution". In: *The Journal of Physical Chemistry A* 113.27, pp. 7707–7713.

Saunders, R. W., R. Kumar, S. M. MacDonald, and J. M. C. Plane (Nov. 6, 2012). "Insights into the Photochemical Transformation of Iodine in Aqueous Systems: Humic Acid Photosensitized Reduction of Iodate". In: *Environmental Science & Technology* 46.21, pp. 11854–11861.

Schmitz, G. and S. Furrow (Mar. 28, 2012). “Kinetics of the iodate reduction by hydrogen peroxide and relation with the Briggs–Rauscher and Bray–Liebhafsky oscillating reactions”. In: *Physical Chemistry Chemical Physics* 14.16, pp. 5711–5717.

Steffen, A., T. Douglas, M. Amyot, P. Ariya, K. Aspmo, T. Berg, J. Bottenheim, S. Brooks, F. Cobbett, A. Dastoor, A. Dommergue, R. Ebinghaus, C. Ferrari, K. Gardfeldt, M. E. Goodsite, D. Lean, A. J. Poulain, C. Scherz, H. Skov, J. Sommar, and C. Temme (Mar. 12, 2008). “A synthesis of atmospheric mercury depletion event chemistry in the atmosphere and snow”. In: *Atmospheric Chemistry and Physics* 8.6, pp. 1445–1482.

Whitehead, D. C. (Jan. 1, 1984). “The distribution and transformations of iodine in the environment”. In: *Environment International* 10.4, pp. 321–339.

Winter, J. M. and B. S. Moore (July 10, 2009). “Exploring the Chemistry and Biology of Vanadium-dependent Haloperoxidases*”. In: *Journal of Biological Chemistry* 284.28, pp. 18577–18581.

Zheng, W., S. K. Papiernik, M. Guo, and S. R. Yates (Jan. 1, 2003). “Accelerated Degradation of Methyl Iodide by Agrochemicals”. In: *Journal of Agricultural and Food Chemistry* 51.3, pp. 673–679.

Acronyms

BLM Bla Bla bla 20, 26, *see Glossary:* Bray-Liebhafsky mechanism
BRM Bla Bla bla 20, 26, *see Glossary:* Briggs-Rauscher mechanism
BTCA 1,2,3,4 butanetetracarboxylic acid 22, 27
BTOF bipolar time-of-flight 9
BTOF-CIMS bipolar time-of-flight chemical ionisation mass spectrometer 9
BVOC biogenic volatile organic compound 8

CA Citric acid 22, 27
CE-DOAS Cavity-Enhanced Differential Optical Absorbtion Spectroscopy 22, 27, *see Glossary:* CE-DOAS
CIMS chemical ionisation mass spectrometer 9
Cit Citrate 22, 28
CNN cloud condensation nucleus 19, 25
CPC Condensation particle counter 10, 11
CWFTR Coated Wall Flow Tube Reactor 22, 27, *see Glossary:* CWFTR

DMA Differential mobility analyser 11
DOAS Differential Optical Absorbtion Spectroscopy *see Glossary:* DOAS

Fe-Cit iron(III)-citrate 22, 27, 28

HA Humic acid 19–21, 25–27
HOM Highly oxidised organic molecule 21, 27

IOP Iodine oxide particle 18, 19, 24, 25
IR Infra red 19, 25

LCP Bla Bla bla 20, 26, *see Glossary:* Le Chatelier's principle (LCP)
LMCT Bla Bla bla 22, 28
LVOC low-volatility organic compound 10

MFC Mass flow controller 9

NPOC Non-purgeable organic carbon 11

OFR oxidation flow reactor 5, 9, 10
OVOC oxygenated volatile organic compound 10, 22, 27

POA primary organic aerosol 21, 27
PSI Paul-Scherrer Institute 9

RIS Reactive Iodine Species 18, 24
ROS Bla Bla bla *see Glossary:* ROS

SMPS Scanning mobility particle sizer 10, 11
SOA secondary organic aerosol 5, 9, 10, 21, 27
SOI Soluble organic iodine 18–20, 24–26

TOC Total organic carbon 5, 9, 11

UFAP ultrafine aerosol particle 19, 25
UV Ultraviolet light 9
UV-A Ultraviolet-A light 19, 25

VIS Visible light 19, 22, 25, 28
VOC Volatile Organic Compound 7–11, 16, 21, 27
VOIC Volatile organic iodine compound 17, 18, 23, 24, 35

List of Symbols

Symbol	Description	Unit
χ	atmospheric mixing ratio	pptv
λ	Wavelength	nm
$\overset{*}{m}$	Mass flow rate	$\mathrm{kg\,s^{-1}}$
pH	Measure of acidity of a solution: $\mathrm{pH} \coloneqq -\log_{10}\left[\mathrm{H^+(aq)}\right]$	
$\overset{*}{V}$	Volumetric flow rate	$\mathrm{m^3\,s^{-1}}$

List of Species

Name	Comment	Formula
α-pinene	2,6,6-trimethylbicyclo[3.1.1]hept-2-ene. Two enantiomers exist.	$C_{10}H_{16}$
β-pinene	6,6-dimethyl-2-methylidenebicyclo[3.1.1]heptane	$C_{10}H_{16}$
Bromide		Br^-
Methyl iodide		CH_3I
Hydrogen ion		H^+
Hydrogen peroxide		H_2O_2
Water (dihydrogen oxide)		H_2O
Peroxide radical		$HO_2^\bullet$
Hypoiodous acid		HOI
Hydrogen oxide radical	Chemical family: $HO_x \coloneqq HO_2^\bullet + HO^\bullet$	HO_x
Iodide		I^-
Iodine radical		$I^\bullet$
Molecular iodine		I_2
Iodine monoxide radical		$IO^\bullet$
Iodine dioxide		IO_2
Iodate		IO_3^-
Iodine oxygen nitrite		$IONO_2$
isoprene	2-metyhl-1,3-butadiene	C_5H_8
Iodine radical species	Chemical family: $I_x \coloneqq I^\bullet + IO^\bullet$	I_x
Total inorganic iodine	Chemical family: $I_y \coloneqq I^\bullet + IO^\bullet + IO_2 + HOI + HI + INO + INO_2 + IONO_2 + 2I_2 + ICl + IBr + 2I_2O_2 + 2I_2O_3 + 2I_2O_4$	I_y
Limonene	1-methyl-4-(prop-1-en-2-yl)cyclohex-1-ene	$C_{10}H_{16}$
Molecular nitrogen		N_2
Sodium iodate		$NaIO_3$
Nitrogen dioxide		NO_2
Nitrogen monoxide		NO
Nitrous oxide	Chemical family: $NO_x \coloneqq NO_2 + NO$	NO_x
Oxygen radical (singlet-D)		$O(^1D)^\bullet$
Molecular oxygen		O_2
Ozone		O_3
Hydroxyl radical		$HO^\bullet$
VOIC		RI_n

Glossary

Bray-Liebhafsky mechanism Bla bla bla 20,
Briggs-Rauscher mechanism Bla bla bla 20,

Chromophore Describtoip 19–22, 25–28
CWFTR blabla 22,

Le Chatelier's principle (LCP) Bla bla bla 20,

Matrix (chem.) The components of a solution that are not specifically alanysed but that may significantly alter the behaviour of the substance to be analysed, for instance through matrix effects. *see* matrix effect
matrix effect The effect that matrix has on the analysis and its outcome 22, 27

DOAS Description
CE-DOAS Bla 22,, *see* DOAS

Index

B
Bray-Liebhafsky mechanism . . . 20, **36**
Briggs-Rauscher mechanism . . . 20, **36**

C
Chromophore 19–22, 25–28, **36**
coated wall flow tube 22, **36**

L
Le Chatelier's principle 20, **36**

M
matrix
effect 22, 27, **36**
film **36**

S
Spectroscopy
differential optical absorbtion
cavity-enhanced 22, **36**
differential optical absorbtion **36**